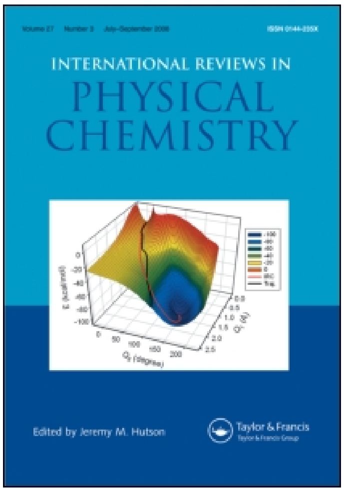

International Reviews in Physical Chemistry
Publication details, including instructions for authors and subscription information:
http://www.informaworld.com/smpp/title~content=t713724383

The Cotton-Mouton effect in gases: Experiment and theory

Carlo Rizzo; Antonio Rizzo; David M. Bishop

To cite this Article Rizzo, Carlo , Rizzo, Antonio and Bishop, David M.(1997) 'The Cotton-Mouton effect in gases: Experiment and theory', International Reviews in Physical Chemistry, 16: 1, 81 — 111
To link to this Article: DOI: 10.1080/014423597230316
URL: http://dx.doi.org/10.1080/014423597230316

INTERNATIONAL REVIEWS IN PHYSICAL CHEMISTRY, 1997, VOL. 16, NO. 1, 81–111

The Cotton–Mouton effect in gases: experiment and theory

by CARLO RIZZO†
Istituto Nazionale di Fisica Nucleare, Laboratori Nazionali, via Romea 4, I-35020
Legnaro, Padova, Italy

ANTONIO RIZZO
Istituto di Chimica Quantistica ed Energetica Molecolare, Consiglio Nazionale
delle Ricerche, via Risorgimento 35, I-56126 Pisa, Italy

and DAVID M. BISHOP
Department of Chemistry, University of Ottawa, Ottawa, Canada K1N 6N5

When polarized light passes through a material in the presence of a strong magnetic field, birefringence is observed. This is known as the Cotton–Mouton effect. Owing to the increasing sophistication of both experimental and computational techniques, this particular aspect of magneto-optics has been investigated increasingly in the last few years. In this review the basic facts concerning both experiment and theory are discussed and tables summarizing all currently known gas-phase data are presented.

1. Introduction

At the turn of the century it was experimentally shown that gases have a weak birefringence when polarized light passes through them in the presence of a strong magnetic field normal to the direction of the light. This magnetic-field-induced birefringence is called the Cotton–Mouton effect (CME), since it was first investigated in detail by A. Cotton and H. Mouton [1] in 1905. In fact, Kerr [2] had observed the weak birefringence of a suspension of Fe_3O_4 in water in a magnetic field in 1901 and Majorana [3] a year later had witnessed the same behaviour in colloidal solutions of iron. Nonetheless, the work of Cotton and Mouton was the first complete study of the phenomenon and it is known by their names. They recognized the analogy with the Kerr [4] effect, electric-field-induced birefringence, and were able to separate the magnetic birefringence signal from the stronger Faraday effect signal, which is the rotation of the polarization vector by a magnetic field applied in the direction of the light [5]. The new effect was extremely small and measurements in *gases* before the first systematic work of Buckingham *et al.* [6] in 1967 were very few and far between [7–10]. Investigations concerned benzene vapour [7], hydrogen, nitrogen, nitrogen monoxide and oxygen [8, 9] at high pressures, and ethane [10]. Since 1967, many more papers concerning the effect in gases have been published [11–33] and CME experiments have been employed as sensitive probes of the electromagnetic properties of molecules. For example, the magnetizability and electric polarizability anisotropies may be obtained from CME experiments [12, 17]. CME is a particularly valuable source of information for the magnetizability anisotropies of non-polar molecules, as these species do not

---

† Permanent address: Istituto Nazionale di Fisica Nucleare, Sezione di Trieste, Via Valerio 2, I-34127 Trieste, Italy.

show a microwave spectroscopic rotational Zeeman effect [12, 15]. Interest in the CME has grown with the increase in the technical possibilities in optics. It is to be noted that the same effect should also occur, at an extremely low level, when polarized light propagates in vacuum in the presence of a strong transverse magnetic field because of vacuum fluctuations [34]. This provides a further justification for efforts to study the phenomenon in gases, since in recent years there has been a growing interest in developing very sensitive equipment to measure vacuum magnetic birefringence [35–38]. For this type of experiment, CME measurements are a good test of the overall sensitivity of the apparatus. Moreover the CME of the residual gas in a vacuum tube can give rise to unwanted systematic effects, whose amplitude should be known prior to setting the vacuum requirements of the experiment.

The first theoretical treatment of the CME dates from 1910 [39] but the decisive contribution to the understanding of the topic was given by Buckingham and Pople [40] in 1956. Since then, different aspects of the theory have been studied in detail [41–44] and research has been undertaken in quantum-chemical laboratories in several countries to produce reliable estimates of the effect. The list of references is increasing [45–65], with a formidable number of theoretical papers in the last decade. The field is expanding, in parallel, with the advances which have been made in calculations of other nonlinear optical properties in recent years [66].

Some aspects of the CME have already been treated elsewhere. Very often the Kerr effect and the CME are treated together. A chapter entitled ‘The Kerr effect and related phenomena’ in the book by Böttcher and Bordewijk [67] includes optical magnetically induced birefringence. A review by Williams [68] deals with both the optical Kerr and the Cotton–Mouton effects in solutions. It complements this work by giving complete references and a detailed account of the state of the art for CME in solutions and discusses the problems arising when one considers dense fluids. A section of a review on the aspects of nonlinear optical calculations in atoms and molecules written by one of us [66] also discusses the CME.

In this article we review the literature concerning the CME in gases. Tables are given of both experimental and theoretical results and a critical assessment of both experiment and computational results is attempted. CME is in some respects quite a unique field, since the theoretical models, the computational techniques and the experiments are put to a severe test. The intention of this work is to provide experimentalists and theoretical chemists alike with a collection of data, as complete as possible, in the hope of furthering a better exchange of information between them.

2. Experiment

The first comprehensive measurements of the CME in gases were reported in [6]. The presence of a strong magnetic field B† changes the index of refraction with respect to the zero-field case for light propagating in a medium. The change depends on the direction of the polarization of the light. If $n_\parallel$ is the index of refraction for light linearly polarized parallel to the magnetic field and $n_\perp$ the index for the polarization normal to the magnetic field, the birefringence δ shown by the medium after the light has propagated an optical path L is

$$\delta = 2\pi \frac{L}{\lambda}(n_\parallel - n_\perp)\sin(2\theta) = 2\pi \frac{L}{\lambda}\Delta n \sin(2\theta), \tag{1}$$

---

† Strictly speaking B indicates the magnetic induction or magnetic flux density.

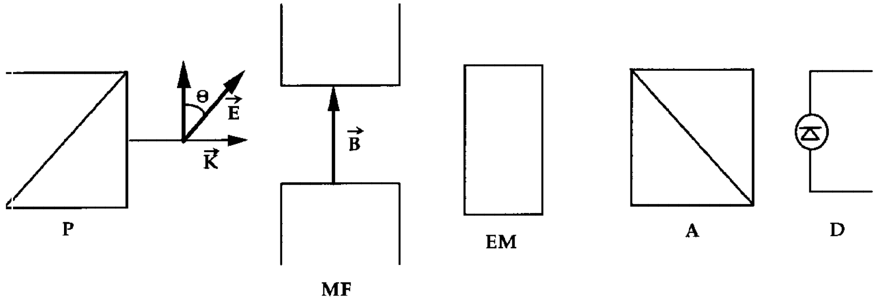

Figure 1. A scheme for an experimental set-up: P, polarizer prism; MF, magnetic field region; EM, ellipticity modulator; A, analyser prism; D, photodiode.

where θ is the angle between the light polarization and the direction of the transverse magnetic field and λ is the wavelength of the light. Δn is therefore the physical quantity to which the CME is related.

Up to now, all researchers have obtained Δn by the measurement of the ellipticity Ψ acquired by a polarized light beam going through the birefringent medium. In the case of a very small birefringence the ellipticity Ψ is related to the birefringence by the formula [69]

$$\Psi \approx \frac{\delta}{2} = \pi \frac{L}{\lambda} \Delta n \sin(2\theta). \tag{2}$$

Since the pioneering work of Buckingham *et al.* [6] the CME of almost 40 different gas species has been measured. The homodyne detection technique, on which the original apparatus in [6] was based, has been used by several workers [11–13, 15–17, 19–22, 25–28, 31–33]. The ellipticity to be measured is static and to increase the sensitivity of the apparatus an ellipticity modulator is introduced in the optical path. The experimental technique has been described in detail in [68] and has been very successful. For example, Hüttner *et al.* [25] measured, in 1987, the CME of hydrogen corresponding to a Δn of about 9×10^{-15} at standard temperature and pressure (STP) with a magnetic field $B = 1$ T. The experimental error in Δn was about $2{\cdot}5 \times 10^{-16}$. Up to now, this is the lowest value of Δn that has been published using this type of apparatus. Its main limitation comes from the total static birefringence present in the optical system. This static birefringence is typically between 10^{-4} and 10^{-5} rad [68].

A different apparatus, based essentially on the experimental method proposed in 1979 by Iacopini and Zavattini [70] to measure the vacuum magnetic birefringence [34], has been used by several groups [14, 18, 23, 29, 30]. Quantum electrodynamics predicts that a vacuum should show magnetic birefringence. The effect is so small that a direct measurement has not yet been possible. In the case of this very elementary 'gas', in the optical region and for a magnetic field $B \ll 4 \times 10^{9}$ T, the field strength at which real electron–positron pairs start to form, Δn is independent of λ and temperature. The predicted value for $B = 1$ T is $\Delta n = 4{\cdot}0 \times 10^{-24}$, that is about eight orders of magnitude smaller than the smallest anisotropies observed in gases.

The CME of helium, the smallest CME so far found [30], has been measured using this technique. At STP and with $B = 1$ T it corresponds to a Δn of about 2×10^{-16}. Noise levels corresponding to Δn of about 2×10^{-17} were also observed [29, 30]. This sensitivity was obtained by modulating the applied magnetic field and using the heterodyne signal detection technique. In [29] a sensitivity Ψ_{sens} of 10^{-8} rad $\mathrm{s}^{1/2}$ is

Table 1. Relevant spectral components of the signal as given in equation (3).

Frequency	Fourier component	Amplitude	Phase
0	Dc	$\sigma^2 + \varphi_0^2/2$	
ω	I_ω	$2\Gamma\varphi_0$	θ_0
$\omega \pm \Omega$	$I_\pm$	$\Psi_0\,\varphi_0$	$\theta_\pm = \theta_0 \pm \theta_\Psi$
2ω	$I_{2\omega}$	$\varphi_0^2/2$	$2\theta_\Psi$

quoted†. This means that after a data integration time $t = (\Psi_{\mathrm{sens}} / \Psi)^2$ the effect can be measured with a signal-to-noise ratio equal to one. With $\Psi_{\mathrm{sens}} \approx 10^{-8}$ rad $\mathrm{s}^{\frac{1}{2}}$, $B = 1$ T, $L = 1$ m, $\lambda = 5145$ Å and $\theta = 45°$, for the helium gas at STP, t is about 100 s.

In figure 1 a scheme for an experimental set-up designed to use the heterodyne technique is shown. A laser beam is linearly polarized by a polarizer prism P. The angle between the field B and the radiation field E is θ. Passing through the magnetic field region the light acquires an ellipticity $\Psi(t)$. Let us assume that $\Psi(t)$ can be written as $\Psi(t) = \Psi_0 \cos(2\pi\Omega t + \theta_\Psi)$. The radiation then goes through the ellipticity modulator, an optical device that gives to the beam an ellipticity φ ($\gg \Psi$), so that we can assume that $\varphi = \varphi_0 \cos(2\pi\omega t + \theta_\varphi)$. The polarization of the beam is finally analysed by a polarizer prism A crossed at the maximum extinction σ^2 with the polarizer prism P.

Any optical element also acts as a birefringence medium. To take this effect into account we introduce the static ellipticity Γ ($< \sigma$). The light intensity I seen by the photodiode D can be written as

$$I = I_0[\sigma^2 + (\Psi + \varphi + \Gamma)^2], \tag{3}$$

where I_0 is the light intensity before the radiation hits the analyser A. The photodiode converts the intensity I into a current signal, whose power spectrum is studied via Fourier transform techniques. In table 1 we list the amplitudes and the phases of the relevant spectral components of the signal as indicated by equation (3). The ellipticity Ψ_0 can be extracted from the formula

$$\frac{\Psi_0}{\varphi_0} = \frac{I_+}{2I_{2\omega}} = \frac{I_-}{2I_{2\omega}}. \tag{4}$$

Since one measures directly only the ratio of I_+ (I_-) to $I_{2\omega}$, Ψ_0 is not known absolutely, but only relative to φ_0, the ellipticity modulation amplitude. Therefore φ_0 needs to be known to a precision higher than that to which Ψ_0 is measured; otherwise the error in Ψ_0 will be dominated by that in φ_0. The phase of the CME, that is the sign of the effect, is given by

$$\theta_\Psi = \frac{(\theta_+ - \theta_-)}{2}. \tag{5}$$

The main advantage of this method is to shift the frequency of the Fourier component linear in Ψ away from the I_ω components, owing to the modulation of the effect at the frequency Ω. When no modulation is present, the measurement is limited by the value of the static ellipticity Γ, since the value of the I_ω component is a sum of Γ and Ψ_0. This is the typical case for the homodyne technique used in [6]. However,

---

† In this review we adhere to the IUPAC recommendations on the use of units. The experimentalist will notice that we employ, in general, $\mathrm{s}^{\frac{1}{2}}$ in place of the usual $\mathrm{Hz}^{-\frac{1}{2}}$, and $\mathrm{s}^{-\frac{1}{2}}$ for $\mathrm{Hz}/\mathrm{Hz}^{\frac{1}{2}}$.

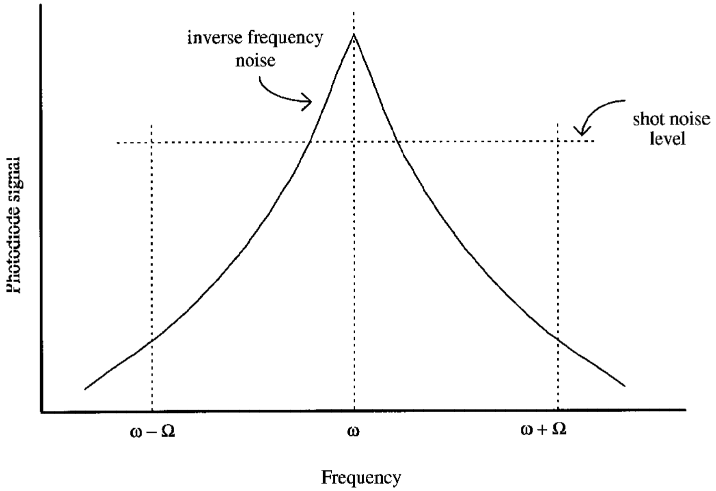

Figure 2. A typical frequency spectrum around ω.

note that, although the field B was not modulated in [6], it could be reversed so that the CME was separated from genuinely static birefringences (from windows etc.), providing valuable discrimination.

When Ψ is modulated, the limiting noise level comes mainly from the inverse frequency noise around the I_ω component and from the quantum noise due to the corpuscular nature of light (shot noise) [71]. Figure 2 shows a typical frequency spectrum around the frequency ω. When all the other experimental parameters are fixed, the frequency Ω should be chosen so that the components I_+ and I_- at $\omega + \Omega$ and $\omega - \Omega$ respectively are in a frequency region where the shot noise is predominant. In practice, Ω should be as large as possible.

The shot noise due to the Poisson distribution of the photon counting is proportional to the square root of the number of photons seen by the photodiode D per second, that is

$$i_{\text{shot noise}} \propto \left(\frac{2e^2 I_0 (\sigma^2 + \varphi_0^2/2) q}{h\nu} \right)^{\frac{1}{2}}, \tag{6}$$

Where ν is the frequency of the light, q is the quantum efficiency of the photodiode, e is the electron charge and h is the Planck constant. The rate of photons corresponding to the signal seen by the photodiode D is proportional to $I_\pm$:

$$i_{\text{signal}} \propto \frac{eI_\pm q}{h\nu} = \frac{eI_0 \Psi_0 \varphi_0 q}{h\nu}. \tag{7}$$

The signal-to-noise ratio is therefore

$$\frac{i_{\text{signal}}}{i_{\text{shot noise}}} = \left(\frac{I_0 \Psi_0^2 \varphi_0^2}{(2\sigma^2 + \varphi_0^2) h\nu} q \right)^{\frac{1}{2}}. \tag{8}$$

Optimal working conditions thus imply that $\sigma^2 \ll \varphi_0^2/2$, that is the extinction should be as low as possible (σ^2 of the order of 10^{-7} has been obtained [29]) while φ_0 should be kept larger than 10^{-3} rad.

A Faraday cell and a quarter-wave plate have been successfully used to give a modulated, stable and sufficiently high value of φ_0 [29]. A Faraday cell can be made of standard glass (e.g. BK7) and put in a modulated magnetic field, whose direction is parallel to that of propagation of the light beam. The resulting Faraday effect [5] in the glass rotates the light polarization vector at the same frequency at which the applied magnetic field is modulated. The magnetic field is usually provided by a solenoid and modulation is obtained by varying the amplitude of the current in the electrical circuit. The quarter-wave plate, when properly aligned, transforms the rotation of the polarization vector for the required φ ellipticity. By imposing the condition of a signal-to-noise ratio equal to one, the expression for the sensitivity Ψ_{sens} is

$$\Psi_{\text{sens}} = \left(\frac{h\nu}{I_0 q}\right)^{\frac{1}{2}}. \tag{9}$$

With $I_0 = 10$ mW $= 1 \times 10^5$ erg s^{-1}, $q = 0{\cdot}5$ and $\nu = 5{\cdot}8 \times 10^{14}$ s^{-1} ($\lambda = 5140$ Å), Ψ_{sens} can be as low as 9×10^{-9} rad s$^{\frac{1}{2}}$.

Different techniques have been proposed and tested to increase the optical path in the magnetic field region. In [29, 30] a multipass optical cavity [72] was employed. This consists of two curved dielectric multilayer interferometric mirrors. The light passes through a hole in the centre of one of the mirrors and after multiple reflections it exits the cavity through the same hole. For the CME measurement on neon [29] the light beam made 36 passes in the cavity but, for the attempt to measure the CME of vacuum, more than 500 transversals were made by slightly deforming one of the mirrors [36]. The main problem with this kind of optical cavity is that a large magnetic volume is necessary in order to have a high number of passes, since the beam never goes along the same path twice inside the cavity. This is one of the reasons for suggesting the use of resonant Fabry–Pérot optical cavities [69] for ellipsometric measurements [37]. Fabry–Pérot cavities, as multipass optical cavities, consist of two dielectric multilayer interferometric mirrors. Light enters the cavity directly through the mirror substrate and at resonance it is concentrated on the cavity axis. Resonance is obtained when the condition

$$\frac{m\lambda}{2} = nL \tag{10}$$

is met. In equation (10), m is an integer (the order of interference), λ is the wavelength of the light, L is the length of the cavity and n is the refractive index of the medium inside the cavity.

The use of the Fabry–Pérot cavity increases the optical path by the factor α (amplification factor) [73] where

$$\alpha = \frac{1+R}{1-R}. \tag{11}$$

Here R is the reflectivity of the mirror (assumed to be equal for the two mirrors). If $R \approx 1$, then

$$\alpha = \frac{2\mathscr{F}}{\pi}, \tag{12}$$

where $\mathscr{F} = R^{\frac{1}{2}}/(1-R)$ is the so-called finesse of the Fabry–Pérot cavity [69]. Finesses up to 2×10^6 have been measured in a cavity of few millimetres length [74]. It would be preferable to have both a high $\mathscr{F}$ and a high L, so that the resulting optical path

$L' = \alpha n L$ might be as long as possible. This concept is represented by the parameter Q, the cavity quality factor, which can be written as

$$Q = \pi \frac{nL\alpha}{\lambda} = \pi \frac{L'}{\lambda}. \tag{13}$$

Quality factors up to 5×10^{11}, corresponding to a finesse $\mathscr{F}$ of about $1{\cdot}57 \times 10^{5}$ for a cavity length $L = 180$ cm have been achieved [75]. This result was found with a residual pressure of a few millibars in the cavity. To obtain a high amplification factor α, the attenuation of light caused by the presence of the gas needs to be negligible when compared with the intrinsic losses on the mirror reflecting surface. This puts, in principle, a limitation on the maximum pressure of the gas sample, depending on the wavelength of the light and the gas itself. For most gases, however, even a small amplification factor is generally enough to guarantee a high-precision measurement.

To obtain a stable Fabry–Pérot cavity, a high relative stability between the frequency of the laser and the resonant frequency of the cavity, given by $\nu_{\mathrm{c}} = mc/2nL$, needs to be reached ($c$ is the velocity of light). This can be done via electronic feedback, by adjusting the length of the cavity or the frequency of the laser. Good relative-frequency stability can be obtained by using the Pound–Drever locking technique [76] and the recently commercially available neodymium-doped yttrium aluminium garnet laser (Nd : YAG) (non-planar ring oscillator, NPRO) [77, 78]. This laser source was designed to be tuned to a wide range around its central frequency of $2{\cdot}8 \times 10^{14}$ Hz ($\lambda = 10\,640$ Å). Spectral densities of the frequency difference between the laser and the cavity lower than 10^{-3} $\mathrm{s}^{-\frac{1}{2}}$ in the frequency range 1–500 Hz can be achieved [79]. Using these new experimental techniques one should be able to measure Δn directly [38].

Let us assume that the apparatus is made of a Fabry–Pérot cavity, in which a gas sample is present, frequency locked to a frequency-stabilized laser source. The laser light is linearly polarized by a polarizer prism before entering the cavity. The locking circuit provides what is called an 'error signal', which is a voltage signal proportional to $\Delta\nu$, the difference between the laser and the cavity frequencies. Acting on the laser, the same circuit maintains $\Delta\nu$ around zero. Let us assume, for simplicity, that the entire optical path L is in the magnetic region, and that the transverse dipole field $\boldsymbol{B}$ rotates around the propagation direction of the linearly polarized light beam with a frequency $\Omega/2$ and phase $\theta_{\Omega}/2$. Under these conditions the light sees a modulated refraction index $n(t)$:

$$\begin{aligned} n(t) &= \frac{n_{\parallel} - n_{\perp}}{2} \cos(2\pi\Omega t + \theta_{\Omega}) + \frac{n_{\parallel} + n_{\perp}}{2} \\ &= \frac{\Delta n}{2} \cos(2\pi\Omega t + \theta_{\Omega}) + n_0 \\ &= n_0 \left(1 + \frac{\Delta n}{2n_0} \cos(2\pi\Omega t + \theta_{\Omega}) \right). \end{aligned} \tag{14}$$

Since $\Delta n / 2n_0 \ll 1$, the resulting $\nu_{\mathrm{c}}(t)$ will be

$$\begin{aligned} \nu_{\mathrm{c}}(\mathrm{t}) &\approx \frac{mc}{2n_0 L} \left(1 - \frac{\Delta n}{2n_0} \cos(2\pi\Omega t + \theta_{\Omega}) \right) \\ &= \nu_0 \left(1 - \frac{\Delta n}{2n_0} \cos(2\pi\Omega t + \theta_{\Omega}) \right), \end{aligned} \tag{15}$$

and finally

$$\frac{\Delta\nu(t)}{\nu_0} \approx \frac{\nu_0 - \nu(t)}{\nu_0} = \frac{\Delta n}{2n_0}\cos(2\pi\Omega t + \theta_\Omega). \tag{16}$$

To estimate the sensitivity of this kind of experiment, let us assume that $\Omega = 1$ Hz and that the spectral density $\Delta\nu_n$ of the difference between the laser and the cavity is of the order of $10^{-3}\ \mathrm{s}^{-\frac{1}{2}}$. If $\nu_0 = 2{\cdot}8 \times 10^{14}$ Hz, one obtains $\Delta\nu_n/\nu_0 = 3{\cdot}6 \times 10^{-18}\ \mathrm{s}^{\frac{1}{2}}$. The sensitivity of $\Delta n/n_0$ is therefore $7{\cdot}2 \times 10^{-18}\ \mathrm{s}^{\frac{1}{2}}$. This means that the CME of helium at STP with a magnetic field $B = 1$ T, could be observed in a few milliseconds of integration time, with a signal-to-noise ratio of about one.

In the last few years the effort to build ever larger accelerators for high-energy particle physics has led to the development of superconducting magnets able to reach fields of about 10 T in a magnetic volume of length several metres and section several square centimetres [80]. Superconducting magnets are electromagnets based on coils built with materials that, at temperatures lower than 4 K, exhibit an electric resistance near zero and are thus capable of withstanding currents of several thousands of amperes. Obviously, owing to the exceedingly high construction and maintenance costs, superconducting magnets are available only for research groups at national and international research laboratories. The studies in [29, 30] were carried out in such laboratories, where there was access to two superconducting magnets. In the following discussion, however, a suggestion is made for a feasible 'desktop' CME experiment based on permanent magnets. Nonetheless, the problem of modulating the ellipticity Ψ remains and, as we have seen, modulation is also necessary for the direct measurement of Δn.

In [14, 29, 30] the amplitude of the magnetic induction field B was changed by modulating the magnet driving current. Using superconducting magnets, the modulating frequencies Ω in [29, 30] were 78•125 and 30•157 mHz respectively, and the magnetic field flux was modulated between 1•94 and 2•48 T. In [14], where a standard electromagnet was employed, the field could be modulated between about 0 and 0•3 T at a frequency of 0•397 Hz. An alternative set-up which enabled higher Ω modulation frequencies to be reached was employed in [18, 23]. The whole 0•54 T dipole electromagnet was rotated at a frequency Ω' of 0•900 Hz in [18] and 1•3125 Hz in [23]. The angle θ between the polarization of light and the magnetic induction field B then becomes

$$\theta = 2\pi\Omega' t + \theta_{\Omega'}. \tag{17}$$

Using equation (2) it is apparent that Ψ is modulated at a frequency Ω which is twice the rotation frequency Ω' of the magnet and that $\theta_\Psi = 2\theta_{\Omega'}$. The effect can be modulated completely from $-\Psi_0$ to $+\Psi_0$.

One might think that rotating the polarization of the beam instead of rotating the field B would be a much easier way to modulate Ψ. Unfortunately, as already mentioned, any optical element in the apparatus also acts as a birefringence plate. Mirrors, for example, exhibit a local birefringence that in some cases can be as large as 10^{-4} [81]. To avoid measuring the birefringence of the optical elements, every optical element of the experiment (mirrors, polarizers, etc.) would have to be rotated in phase with the polarization direction. This is obviously a difficult task and has not yet been accomplished.

A reasonable and cheap solution to the technical problem connected with the rotation of a large electromagnet could be the use of permanent magnets. Nowadays magnetic materials with residual induction of 1•2–1•3 T are commercially available. They can be machined and assembled to obtain a dipole field of about 1 T in a gap of 5 cm between the poles [82]. Considering that no electrical or cryogenic connection needs to be maintained while in motion, this kind of magnet could easily be rotated at frequencies of several hertz.

In conclusion, a feasible, next-generation CME experiment could be performed with a 10 cm permanent 1 T dipole magnet and a Fabry–Pérot cavity with a finesse of about 3×10^4. The resulting ellipticity would be

$$\Psi = \pi \frac{2\mathscr{F}}{\pi} \frac{L}{\lambda} \Delta n \sin(2\theta) = \pi \alpha \frac{L}{\lambda} \Delta n \sin(2\theta). \tag{18}$$

With $\lambda = 10\,640$ Å, in a sample of helium at 10 mbar and room temperature, $\Psi = 10^{-9}$ rad. With a sensitivity $\Psi_{\mathrm{sens}} = 10^{-8}$ rad $s^{\frac{1}{2}}$, Ψ could be measured in about 100 s, at a signal-to noise ratio of about one.

Sensitivity in ellipticity is not sufficient to guarantee a correct measurement. Good control of pressure, temperature and purity of the gas over the whole magnetic volume during the entire experiment is also necessary. Lack of these controls seems at present to be a possible explanation for the discrepancy between experiment and *ab initio* values for gases such as neon and helium, where the effect is very small; see section 6. In the case of neon, for example, the experimental value [29] is about half the theoretical value [54, 55, 63].

In principle, one could calibrate the apparatus using a calibration gas as was done in [18, 23, 30]. However, the experiment should be performed under exactly the same conditions for the calibration (indicated by the superscript cal) gas as the gas under examination, and the CME of the latter should be related to the CME of the former by the formula

$$\Delta n = {}^{\mathrm{cal}}\Delta n \frac{(CM)}{{}^{\mathrm{cal}}(CM)}, \tag{19}$$

where Δn is the anisotropy of the refractive index under the operating conditions and (CM) indicates the CME in arbitrary units. The calibration gas should satisfy the following two conditions.

1. Its value of Δn should be known with precision either experimentally or from theory.
2. Its effect should be easily measurable with a precision higher than that sought for the unknown gas.

When these conditions are not met, systematic errors can arise. For example, in [18] and [23] the authors use two different values for the same reference quantity, the CME of N_2 at STP; that is the first condition is not met.

Using these arguments it is seen that the best candidate as a calibration gas, helium, is not suitable since, although theory has been able to give an extremely reliable estimate for its Cotton–Mouton constant [52], the CME experiment involving helium is exceedingly difficult [30]. The situation is quite different from the electrical nonlinear optical effects, where the results of calibration-quality calculations on small species such as H_2, D_2 [83] or He [84] have been published, and it is accepted that they may be employed as references for the experiments [66].

Another cause of systematic errors arises when the reference value is given at a temperature T' different from T, that at which the measurements for both the sample and the reference gases are performed. In this case, equation (19) should in principle be rewritten as

$$\Delta n_{T'} = {}^{\text{cal}}\Delta n_{T'} \frac{(CM)_T}{{}^{\text{cal}}(CM)_T} \frac{F(T',T)}{{}^{\text{cal}}F(T',T)}, \tag{20}$$

where $F(T',T)$ are functions which take care of the temperature dependence and subscripts $T(T')$ are added to the observables. Equation (20) obviously reduces to equation (19) for $F(T',T) = {}^{\text{cal}}F(T',T)$. If, for instance, the calibration gas is nitrogen, for which ${}^{\text{cal}}F(T',T)$ is approximately proportional to $(T'/T)^2$, and the other gas is argon, for which $F(T',T)$ is proportional to T'/T, the use of equation (19) leads to a systematic error which should be carefully taken into account. This error may be as large as a few per cent of the value for the observable in [18] and in [23]. However, the experimental error in [18] appears to be larger than this possible systematic error.

3. Theory

The first theoretical description of the molecular orientation induced by an electric or magnetic field, and which is partially responsible for both the Kerr effect and the CME, was given by Langevin [39] in 1910. In fact, 2 years before the appearance of Langevin's paper, Voigt had explained magnetic birefringence as the effect of the action of a magnetic field on the electrons of the sample [85] (the nonlinear effect known as the Voigt effect). Langevin's theory was valid only for perfect gases and it supplemented Voigt's ideas, by introducing the temperature-dependent molecular orientational effect, which is far larger than the deformational effect predicted by Voigt. A few years later Born provided a theory for the CME in gases of molecules of arbitrary symmetry, by introducing magnetic hyperpolarizabilities [86] (see also [87]). An account of these first years of the CME has been given by Beams [88], Cotton [89], Germann and Metz [90] and Partington [91]. The essential reference for the theoretical interpretation of the CME in gases has, however, been given by Buckingham and Pople [40], whose analysis of the subject is, in a sense, an alternative to that of Born [86] and follows closely the one that they had developed to account for the dc Kerr effect [92]. More recently, Kielich [41] has discussed a general equation for the molecular Cotton–Mouton constant, containing factors which make it applicable to gases, gas mixtures, liquids and solutions; Atkins and Miller [42] have published a quantum-field-theoretical formulation of optical birefringence, including CME, and Chang [43] has given a quite general description of the CME using a time-dependent double-perturbation approach which allows for the study of the optical frequency dependence. A quantum-mechanical expression for the Cotton–Mouton constant, applicable to any molecule, and which can be used to account for the effect in a paramagnetic species by including the rotational dependence of the coupling between electronic spin and molecular frame, has been developed by Kling *et al.* [16]. Recent references to different aspects of CME theory have been given in the book by Böttcher and Bordewijk [67] and the reviews of Williams [68] and Bishop [66].

The discussion in the next few paragraphs will be based on the work of Buckingham and Pople [40], who employed a general theory of molecular polarizabilities in the presence of a strong magnetic field to relate the anisotropy of the refractive index Δn to the microscopic properties of the medium. They considered a diamagnetic molecule in a closed-shell ground state, thereby avoiding Zeeman splitting; the effect of optical dispersion was ignored and the translational and rotational molecular degrees of freedom were treated classically. The molecular energy U in a strong uniform external magnetic field B with an electromagnetic field described by the uniform electric field E (the associated magnetic field is neglected) can be expanded in a power series as [93]

$$\begin{aligned} U(\tau, E, B) = {} & U_0 - \mu^{\mathrm{e}}_{\alpha} E_{\alpha} - \tfrac{1}{2}\alpha_{\alpha\beta} E_{\alpha} E_{\beta} - \tfrac{1}{2}\chi_{\alpha\beta} B_{\alpha} B_{\beta} \\ & - \tfrac{1}{2}\xi_{\alpha\beta,\gamma} E_{\alpha} B_{\beta} B_{\gamma} - \tfrac{1}{4}\eta_{\alpha\beta,\gamma\delta} E_{\alpha} E_{\beta} B_{\gamma} B_{\delta} + \mathrm{O}[(E, B)^3]. \end{aligned} \tag{21}$$

Einstein summation is assumed and $\mu^{\mathrm{e}}_{\alpha}$ is the α ($\alpha = x, y, z$) component of the electric dipole moment vector, $\alpha_{\alpha\beta}$ and $\chi_{\alpha\beta}$ are the tensor elements of the static electric polarizability and magnetic susceptibility (magnetizability) respectively, $\xi_{\alpha\beta,\gamma}$ and $\eta_{\alpha\beta,\gamma\delta}$ are elements of the first and second hypermagnetizability tensors, and τ represents all configuration (orientational and positional) parameters. By differentiating equation (21) twice with respect to E the differential electric polarizability is

$$\Pi^{\mathrm{e}}_{\alpha\beta} = \alpha_{\alpha\beta} + \tfrac{1}{2}\eta_{\alpha\beta,\gamma\delta} B_{\gamma} B_{\delta} + \dots . \tag{22}$$

According to the Lorentz–Lorenz (or Clausius–Mossotti) equation [94], the refractive index n of a gas is related to the macroscopic electric susceptibility and thus to the microscopic molecular differential electric polarizability Π^{e} by

$$n^2 \approx \varepsilon = 1 + 4\pi \frac{N_{\mathrm{A}}}{(4\pi\varepsilon_0) V_{\mathrm{m}}} \Pi^{\mathrm{e}}. \tag{23}$$

In equation (23), ε is the dielectric constant, N_{A} is the Avogadro constant and V_{m} is the molar volume. The difference of the refractive indices in the two directions (parallel and perpendicular with respect to B) can be written as

$$n_{\parallel} - n_{\perp} \approx \varepsilon_{\parallel}^{1/2} - \varepsilon_{\perp}^{1/2} \approx 2\pi \frac{N_{\mathrm{A}}}{(4\pi\varepsilon_0) V_{\mathrm{m}}} \overline{\Delta\Pi}^{\mathrm{e}}, \tag{24}$$

where $\overline{\Delta\Pi}^{\mathrm{e}}$ is the difference in the polarizability for the two field directions and the bar denotes an average over a statistical distribution of molecular orientations:

$$\overline{\Delta\Pi}^{\mathrm{e}} = \left(\int \Delta\Pi^{\mathrm{e}}(\tau, B) \exp\{-U(\tau, E, B)/kT\} \, \mathrm{d}\tau \right) \Big/ \left(\int \exp\{-U(\tau, E, B)/kT\} \, \mathrm{d}\tau \right). \tag{25}$$

Here k is the Boltzmann constant, T is the temperature and, introducing the unit vectors $e^{\parallel}_{\alpha}$ and $e^{\perp}_{\alpha}$ in the two directions, parallel and perpendicular to the direction of the magnetic field,

$$\Delta\Pi^{\mathrm{e}}(\tau, B) = \Pi^{\mathrm{e}}_{\alpha\beta}(e^{\parallel}_{\alpha} e^{\parallel}_{\beta} - e^{\perp}_{\alpha} e^{\perp}_{\beta}). \tag{26}$$

Buckingham and Pople [40] defined the molar Cotton–Mouton constant ${}_{\mathrm{m}}C$ as

$${}_{\mathrm{m}}C = \lim_{B \to 0} \left(\frac{2(n_{\parallel} - n_{\perp})(4\pi\varepsilon_0) V_{\mathrm{m}}}{27 B^2} \right) = \frac{2\pi N_{\mathrm{A}}}{27} \left(\frac{\partial^2 \overline{\Delta\Pi}^{\mathrm{e}}}{\partial B^2} \right)_{B=0}. \tag{27}$$

By taking the orientational average they showed that Δn could be written as

$$\begin{aligned} \Delta n = \frac{27 B^2}{2 V_{\mathrm{m}} (4\pi\varepsilon_0)} {}_{\mathrm{m}}C &= \frac{\pi B^2 N_{\mathrm{A}}}{V_m (4\pi\varepsilon_0)} \left(\tfrac{1}{5}(\eta_{\alpha\beta,\alpha\beta} - \tfrac{1}{3}\eta_{\alpha\alpha,\beta\beta}) + \frac{1}{5kT} (\alpha_{\alpha\beta}\chi_{\alpha\beta} - \tfrac{1}{3}\alpha_{\alpha\alpha}\chi_{\beta\beta}) \right) \\ &= \frac{\pi B^2 N_{\mathrm{A}}}{V_{\mathrm{m}} (4\pi\varepsilon_0)} \left(\Delta\eta + \frac{1}{5kT} (\alpha_{\alpha\beta}\chi_{\alpha\beta} - \tfrac{1}{3}\alpha_{\alpha\alpha}\chi_{\beta\beta}) \right). \end{aligned} \tag{28}$$

The hypermagnetizability anisotropy $\Delta\eta$ is defined as

$$\Delta\eta = \tfrac{1}{5}(\eta_{\alpha\beta,\alpha\beta} - \tfrac{1}{3}\eta_{\alpha\alpha,\beta\beta}). \tag{29}$$

For axial molecules,

$$\Delta n = \frac{\pi B^2 N_A}{V_m(4\pi\varepsilon_0)}\left(\Delta\eta + \frac{2}{15kT}\Delta\alpha\Delta\chi\right), \tag{30}$$

where $\Delta\alpha = \alpha_{zz} - \alpha_{xx}$ and $\Delta\chi = \chi_{zz} - \chi_{xx}$, and z and x are molecular axes, the molecule being placed along the z axis. The first term in equations (28) and (30) describes the effect of the magnetic field on the electric polarizability, and it is generally much smaller than the temperature-dependent factor. There are some notable exceptions to this 'rule' (see for instance H_2O [60]). The second term in equations (28) and (30) represents the Langevin temperature-dependent contribution, that is the orientational effect of the external fields on the molecules. The Langevin contribution vanishes exactly for atoms and 'spherical' molecules, that is molecules of cubic or icosahedral symmetry for which the anisotropies of the electric polarizability and magnetizability vanish. In these cases, equation (30) reduces to

$$\Delta n = \frac{\pi B^2 N_A}{V_m(4\pi\varepsilon_0)}\Delta\eta = \frac{\pi B^2 N_A}{V_m(4\pi\varepsilon_0)}(\eta_{zz,zz} - \eta_{zz,xx}) \tag{31}$$

since $\eta_{zz,zz} = \eta_{xx,xx} = \eta_{yy,yy}$ and $\eta_{zz,xx} = \eta_{zz,yy} = \eta_{xx,yy} = \dots$.

The number of non-vanishing independent elements of the hypermagnetizability tensor $\boldsymbol{\eta}$ is, in principle, 36 (and *not* 81), owing to the intrinsic permutability of the α, β and γ, δ indices (i.e. $\eta_{\alpha\beta,\gamma\delta} = \eta_{\beta\alpha,\gamma\delta}$, $\eta_{\alpha\beta,\delta\gamma} = \eta_{\beta\alpha,\delta\gamma}$). Molecular symmetry further reduces this number, since most components vanish and many of the non-vanishing components are related. The number of non-vanishing independent components of $\boldsymbol{\eta}$ for a given molecular symmetry can be determined by group-theoretical techniques [95]. In axial systems, for instance, only six independent non-vanishing components exist [48]:

$$\begin{gathered}
\eta_{xx,xx} = \eta_{yy,yy} \neq \eta_{zz,zz},\\
\eta_{xx,yy} = \eta_{yy,xx},\\
\eta_{xy,xy} = \eta_{xy,yx} = \eta_{yx,yx} = \eta_{yx,xy} = \tfrac{1}{2}(\eta_{xx,xx} - \eta_{xx,yy}) = \tfrac{1}{2}(\eta_{yy,yy} - \eta_{yy,xx}),\\
\eta_{xx,zz} = \eta_{yy,zz},\\
\eta_{xz,xz} = \eta_{xz,zx} = \eta_{yz,yz} = \eta_{yz,zy} = \eta_{zx,zx} = \eta_{zx,xz} = \eta_{zy,zy} = \eta_{zy,yz},\\
\eta_{zz,xx} = \eta_{zz,yy},
\end{gathered} \tag{32}$$

where again z is the internuclear axis and equation (30) becomes

$$\Delta\eta = \tfrac{1}{15}(7\eta_{xx,xx} - 5\eta_{xx,yy} + 2\eta_{zz,zz} - 2\eta_{xx,zz} - 2\eta_{zz,xx} + 12\eta_{xz,xz}). \tag{33}$$

Tables of the non-vanishing independent components of $\boldsymbol{\eta}$ and of their relationships for different molecular symmetries can be deduced from those given for the only slightly more complicated case of the nuclear magnetic shielding polarizabilities by Raynes and Ratcliffe [96].

For an ideal gas, equation (30) can be rewritten as

$$\Delta n = \frac{\pi B^2 P}{4\pi\varepsilon_0}\left(\frac{\Delta\eta}{kT} + \frac{2}{15(kT)^2}\Delta\alpha\Delta\chi\right), \tag{34}$$

where P is the pressure of the gas. The first term depends on the inverse of the temperature while the second depends on the inverse of the square of the temperature. The relative importance of the two terms changes from molecule to molecule. As mentioned before, for H_2O vapour at room temperature the first term appears to be about ten times larger than the second term, while for N_2 under the same conditions the first term contributes only a few per cent to the overall effect [60]. Since in the case of atoms the second term in equation (34) vanishes, Δn shows a pure $1/T$ dependence at constant pressure.

The Cotton–Mouton constant in non-ideal gases has a slightly more complicated dependence on the temperature and on the microscopic properties. The quantum-mechanical analysis of Kling *et al.* [16] becomes essential for molecules with small moments of inertia, where quantum corrections to classical behaviour become important. The reader can find in [16] a detailed derivation of the expression for the Cotton–Mouton constant, as well as a discussion of the limiting behaviour at high temperatures. In the approximation of linear rigid rotors with negligible centrifugal distortion of the molecular parameters, equation (30) becomes [17]

$$\begin{aligned}\Delta n &= \frac{\pi B^2 N_A}{V_m(4\pi\varepsilon_0)}\left(\Delta\eta + \frac{2}{15kT}\left(1-\sigma+\tfrac{8}{15}\sigma^2+\dots\right)\Delta\alpha\Delta\chi\right.\\ &\qquad\left.-\frac{2}{15kT}\left(1-\tfrac{1}{3}\sigma-\tfrac{1}{45}\sigma^2+\dots\right)\frac{g_\perp^2\mu_n^2}{2hB_e}\Delta\alpha\right)\\ &= \frac{\pi B^2 N_A}{V_m(4\pi\varepsilon_0)}\left(\Delta\eta+\frac{2}{15kT}\Delta\alpha\Delta\chi_{\mathrm{eff}}\right),\end{aligned} \tag{35}$$

segment where B_e is the rotational constant, $g_\perp\mu_n$ is the gyromagnetic ratio (μ_n is the nuclear magneton), $\sigma = hB_e/kT$ and

$$\Delta\chi_{\mathrm{eff}} = \left(1-\sigma+\tfrac{8}{15}\sigma^2+\dots\right)\Delta\chi-\left(1-\tfrac{1}{3}\sigma-\tfrac{1}{45}\sigma^2+\dots\right)\frac{g_\perp^2\mu_n^2}{2hB_e}. \tag{36}$$

The first correction term in equation (36) is precisely analogous to that for the corresponding term in the Kerr effect [97] and, even if truncated to the first order in σ, can be quite influential and it affected the results of the CME measurements of N_2 and CO up to one standard deviation [17]. The second term in equation (36) describes the orientational influence of the rotational magnetic moments and is negligible in molecules which do not exhibit large rotational g factors. The case of paramagnetic gases requires a complete quantum-mechanical analysis. Some extra (paramagnetic) terms arise in the expansion of the refractive index, equation (35), and in general these gases exhibit a strong temperature dependence. Examples are seen in the studies of the CME in O_2 [16, 28] and NO [20].

The pressure dependence of Δn is always linear for an ideal gas. The case of a non-ideal gas is treated both theoretically and experimentally in [25]. The Cotton–Mouton constant is expanded in terms of the number N of moles per unit volume. This introduces the Cotton–Mouton virial coefficients A_C, B_C, C_C, … :

$${}_mC = A_C + B_C N + C_C N^2 + \dots . \tag{37}$$

Equation (37) is analogous to the earlier description of the molar Kerr constant ${}_mK$ [98]. The first virial coefficient A_C is the term in equation (27). Expressions for the second virial coefficient B_C can be found in [25, 41]. A detailed experimental study of the density dependence for hydrogen has been given in [25].

It has already been mentioned that in molecular systems the Langevin term in the refractive index anisotropy can be by far the largest contribution. It is related to the electric polarizability and magnetizability anisotropies. There is a vast literature on experiment, theory and computational techniques for these second-order properties. It is beyond our scope to give a detailed discussion of this topic but, since we are concerned with all aspects of the CME in gases, and since we are going to compare experiment and theory, we shall have to introduce estimates of the electric polarizability and magnetizability anisotropies later. Our attention, for the moment, will be focused on the hypermagnetizability $\boldsymbol{\eta}$, a quantity which is far more difficult to compute and much less popular in the scientific literature.

As is implicit in equation (28), Δn depends on the wavelength of the light, owing to the ω ($= 2\pi c/\lambda$) dependence of the microscopic properties η and α [99]. An equation equivalent to that for the energy, equation (21), can be written for the polarization when the fields oscillate. The polarizabilities introduced in equation (21) are then explicitly dependent upon the circular frequencies (ω_j below) of the fields. In particular the hypermagnetizability tensor $\boldsymbol{\eta}$, which is composed, as is $\boldsymbol{\chi}$, of a paramagnetic (indicated by a superscript p) and a diamagnetic (indicated by a superscript d) part, is written as

$$\eta_{\alpha\beta,\gamma\delta}(\omega) = \eta^{\rm p}_{\alpha\beta,\gamma\delta}(-\omega_\sigma;\omega_1,\omega_2,\omega_3) + \eta^{\rm d}_{\alpha\beta,\gamma\delta}(-\omega_\sigma;\omega_1,\omega_2), \tag{38}$$

where $\omega_\sigma = \Sigma_j \omega_j$. In the Cotton–Mouton experiment, equation (38) becomes

$$\eta_{\alpha\beta,\gamma\delta}(\omega) = \eta^{\rm p}_{\alpha\beta,\gamma\delta}(-\omega;\omega,0,0) + \eta^{\rm d}_{\alpha\beta,\gamma\delta}(-\omega;\omega,0). \tag{39}$$

Note that indices α, β are associated with the electric perturbation, while indices γ, δ are associated with the magnetic perturbation.

Explicit expressions for $\eta^{\rm p}_{\alpha\beta,\gamma\delta}(-\omega_\sigma;\omega_1,\omega_2,\omega_3)$ and $\eta^{\rm d}_{\alpha\beta,\gamma\delta}(-\omega_\sigma;\omega_1,\omega_2)$ in terms of sum-over-states expansions involving matrix elements of the dipole moment, magnetic moment and diamagnetic magnetizability operators have been given by Bishop *et al.* [50]. Following the perturbative treatment of Orr and Ward [100], and in the presence of the double perturbation,

$$H = -\hat{\mu}^{\rm e}\cdot E - \hat{\mu}^{\rm m}\cdot B - \tfrac{1}{2}B\cdot\hat{\boldsymbol{\chi}}^{\rm d}\cdot B. \tag{40}$$

Bishop *et al.* obtained

$$\begin{aligned}\eta^{\rm p}_{\alpha\beta,\gamma\delta}(-\omega_\sigma;\omega_1,\omega_2,\omega_3) = \frac{1}{\hbar^3}\sum_P\Bigg(&\sum_{m,n,p,(\neq g)}\frac{\langle g|\hat{\mu}^{\rm e}_\alpha|m\rangle\langle m|\hat{\bar{\mu}}^{\rm m}_\delta|n\rangle\langle n|\hat{\bar{\mu}}^{\rm m}_\gamma|p\rangle\langle p|\hat{\mu}^{\rm e}_\beta|g\rangle}{(\omega_{mg}-\omega_\sigma)(\omega_{ng}-\omega_1-\omega_2)(\omega_{pg}-\omega_1)}\\ &-\sum_{m,n(\neq g)}\frac{\langle g|\hat{\mu}^{\rm e}_\alpha|m\rangle\langle m|\hat{\mu}^{\rm m}_\delta|g\rangle\langle g|\hat{\mu}^{\rm m}_\gamma|n\rangle\langle n|\hat{\mu}^{\rm e}_\beta|g\rangle}{(\omega_{mg}-\omega_\sigma)(\omega_{ng}-\omega_1)(\omega_{ng}+\omega_2)}\Bigg),\end{aligned} \tag{41}$$

$$\eta^{\rm d}_{\alpha\beta,\gamma\delta}(-\omega_\sigma;\omega_1,\omega_2) = \frac{1}{\hbar^2}\sum_P\sum_{m,n(\neq g)}\frac{\langle g|\hat{\mu}^{\rm e}_\alpha|m\rangle\langle m|\overline{\chi}^{\rm d}_{\gamma\delta}|n\rangle\langle n|\hat{\mu}^{\rm e}_\beta|g\rangle}{(\omega_{mg}-\omega_\sigma)(\omega_{ng}-\omega_1)}, \tag{42}$$

where $\omega_2 = \omega_3 = 0$ in the CME experiment. The dipole moment operator is

$$\hat{\mu}^{\rm e}_\alpha = -|e|\sum_i r^{\rm G}_{i,\alpha}. \tag{43}$$

$r^{\rm G}_{i,\alpha} = (r_{i,\alpha} - R_{{\rm G},\alpha})$ and denotes electronic coordinates with respect to the gauge origin (G), $r_{i,\alpha}$ is the α coordinate for electron i and $R_{{\rm G},\alpha}$ is the α coordinate of the gauge origin. The magnetic moment operator is

$$\hat{\mu}^{\rm m}_\alpha = -\frac{|e|}{2m_{\rm e}}\sum_i l^{\rm G}_{i,\alpha}. \tag{44}$$

Here $l^{\mathrm{G}}_{i,\alpha} = \varepsilon_{\alpha\beta\gamma} r^{\mathrm{G}}_{i,\beta} p_{i,\gamma}$ is the α component of the angular momentum operator of electron i, $\varepsilon_{\alpha\beta\gamma}$ denotes the third-rank alternating tensor, and $p_{i,\gamma}$ is the γ component of the linear momentum operator of electron i. The diamagnetic magnetizability operator is

$$\hat{\chi}^{\mathrm{d}}_{\alpha\beta} = -\frac{|e|^2}{4m_{\mathrm{e}}} \sum_i \left[(r_i - R_{\mathrm{G}})^2 \delta_{\alpha\beta} - r^{\mathrm{G}}_{i,\alpha} r^{\mathrm{G}}_{i,\beta} \right]. \tag{45}$$

In equation (41), Σ_P indicates a sum over all the terms obtained by permutation of the four pairs $(-\omega_\sigma, \hat{\mu}^{\mathrm{e}}_\alpha)$, $(\omega_1, \hat{\mu}^{\mathrm{e}}_\beta)$, $(\omega_2, \hat{\mu}^{\mathrm{m}}_\gamma)$ and $(\omega_3, \hat{\mu}^{\mathrm{m}}_\delta)$. In equation (42), Σ_P indicates a similar permutation of the three pairs $(-\omega_\sigma, \hat{\mu}^{\mathrm{e}}_\alpha)$, $(\omega_1, \hat{\mu}^{\mathrm{e}}_\beta)$ and $(\omega_2, \hat{\chi}^{\mathrm{d}}_{\gamma\delta})$. The bars indicate the fluctuation operator $\bar{\hat{\mu}} = \hat{\mu} - \langle g|\hat{\mu}|g\rangle$, the exclusion of the ground state contribution g in the summations is indicated explicitly, the $|n\rangle$ are the electronic excited-state wavefunctions and $\hbar\omega_{ig} = E_i - E_g$ are the energy differences.

Equations (41) and (42) can also be obtained using the formalism of response theory (see for example [101]). By adopting the notation and conventions of [102] and by neglecting, for simplicity, the dependence on the gauge origin, they can be rewritten as

$$\eta^{\mathrm{p}}_{\alpha\beta,\gamma\delta}(-\omega;\omega,0,0) = -\tfrac{1}{4}\langle\langle r_\alpha; r_\beta, l_\gamma, l_\delta\rangle\rangle_{-\omega:\omega,0,0}, \tag{46}$$

$$\eta^{\mathrm{d}}_{\alpha\beta,\gamma\delta}(-\omega;\omega,0) = -\tfrac{1}{4}\langle\langle r_\alpha; r_\beta, (r^2\delta_{\gamma\delta} - r_\gamma r_\delta)\rangle\rangle_{-\omega:\omega,0}, \tag{47}$$

where the sum over the electrons is implied and the quantities in double angular brackets are appropriate cubic (equation (46)) and quadratic (equation (47)) response functions [102]. All the above equations refer to a diamagnetic species.

Equations (41) and (42) or, equivalently, equations (46) and (47) could be used in principle and were used in practice in some cases, to compute the hypermagnetizability $\boldsymbol{\eta}$. Bishop *et al.* [50] were able, for instance, to study the frequency-dependent hypermagnetizability anisotropy of H_2 and D_2. The recent development of the cubic response approach [63] is also very promising in this respect. Frequency-dependent hypermagnetizability anisotropies of CH_4, NH_3, H_2O, HF [61] and the rare gases and some of their isoelectronic species [63] have been computed using this approach.

In the general case the determination of the paramagnetic contribution to the hypermagnetizability anisotropy proves to be a formidable task but, for systems possessing spherical symmetry and below the first resonant frequency, $\Delta\eta^{\mathrm{p}}$ reduces to the more tractable Cauchy-type moment expansion [51, 52, 103]

$$\Delta\eta^{\mathrm{p}}(\omega) = -\tfrac{1}{4}\frac{\mathrm{d}^2\alpha(-\omega;\omega)}{\mathrm{d}\omega^2} = -\tfrac{1}{4}\sum_{n=0}^{\infty}(2n+1)(2n+2)\,S(-2n-4)\left(\frac{\hbar\omega}{E_{\mathrm{h}}}\right)^{2n}. \tag{48}$$

Here $S(-j)$ indicates the appropriate Cauchy moment (sum rule)

$$S(-j) = \sum_{n(\neq g)} f_n \left(\frac{E_{\mathrm{h}}}{\hbar\omega_{ng}}\right)^j \tag{49}$$

and f_n is the oscillator strength. The connection between the frequency-dependent electric dipole polarizability $\alpha(-\omega;\omega)$ and $\boldsymbol{\eta}$ is explicit in equation (48).

The relation between the diamagnetic hypermagnetizability and the dipole–dipole–quadrupole polarizability [104] was first given by Fowler and Buckingham [48] for $\omega = 0$ and generalized by Bishop *et al.* [50] for the dynamic quantities. The 'traced' dipole–dipole–quadrupole hyperpolarizability is defined as [105, 106]

$$\tilde{B}_{\alpha\beta,\gamma\delta}(\omega) = -\langle\langle r_\alpha; r_\beta, r_\gamma r_\delta\rangle\rangle_{-\omega;\omega,0} \tag{50}$$

and the usual ('traceless') dipole–dipole–quadrupole is

$$B_{\alpha\beta,\gamma\delta}(\omega) = -\langle\langle r_\alpha; r_\beta, (\tfrac{3}{2} r_\gamma r_\delta - \tfrac{1}{2} r^2 \delta_{\gamma\delta})\rangle\rangle_{-\omega;\omega,0}. \tag{51}$$

By comparing with equations (47) it is apparent that

$$\eta^{\mathrm{d}}_{\alpha\beta,\gamma\delta}(\omega) = \tfrac{1}{2}[\tilde{B}_{\alpha\beta,\gamma\delta}(\omega) - B_{\alpha\beta,\gamma\delta}(\omega)], \tag{52}$$

The connections between the traced and traceless tensors defined above have been widely discussed in the literature [104]. When $\gamma \neq \delta$, $\eta^{\mathrm{d}}_{\alpha\beta,\gamma\delta}$ can be expressed in terms of $\boldsymbol{B}$ alone [48], for example for an atom or spherical molecule

$$\eta^{\mathrm{d}}_{xy,xy} = -\tfrac{1}{6}B_{xy,xy} = -\tfrac{1}{8}B, \tag{53}$$

where B is the scalar dynamic dipole–dipole–quadrupole hyperpolarizability. The dynamic diamagnetic hypermagnetizability anisotropy for molecules of arbitrary symmetry can be written as

$$\Delta\eta^{\mathrm{d}}(\omega) = -\tfrac{1}{30}B_{\alpha\beta,\alpha\beta}(\omega) = -\tfrac{1}{4}\bar{B}(\omega), \tag{54}$$

where $\bar{B}(\omega)$ is the isotropically averaged dynamic B polarizability.

The dependence of $\Delta\eta$ on λ cannot in general be easily predicted, but in the optical region the variation in $\Delta\eta$ should, in principle, be small, especially if compared with error in the experimental value. For example, in the case of argon, data taken from both [55] and [58] show that $\Delta\eta$ changes by less than 1% when λ varies between 10 640 and 4880 Å.

Molecular vibrations affect nonlinear optical properties, such as the hypermagnetizabilities discussed here, via both the zero-point vibrational averaging of the calculated properties and the effect of the radiation on the vibrational motion. This last interaction gives rise to the vibrational hypermagnetizabilities. This whole subject is receiving increasing consideration, especially since vibrational contributions to physical observables and to the magnetically induced birefringence in particular are often far from negligible. A review of the literature and a broad discussion of the topic has been given by one of us elsewhere [66, 104]. Only a brief summary of the main points is given here.

Electronic state properties in molecules are usually computed in the fixed nuclei Born–Oppenheimer (BO) approximation. A comparison of theory and experiment requires that the results obtained at fixed internuclear distances be corrected for vibrational effects. The zero-point vibrational correction of a given electronic property P can be estimated via the expectation value (generally over the ground vibrational state)

$$\bar{P} = \langle \upsilon(0)|P|\upsilon(0)\rangle. \tag{55}$$

For diatomic molecules the ground-state vibrational wavefunction $\upsilon(0)$ is often obtained using the Numerov–Cooley method [107, 108]. If we wish to take rotation into account, then we write, for diatomics [50],

$$\overline{\Delta\eta} = \sum_J \rho(J)\langle\upsilon(0,J)|\Delta\eta|\upsilon(0,J)\rangle, \tag{56}$$

where the $\upsilon(0,J)$ rovibrational wavefunctions are obtained by a Numerov–Cooley solution of the rovibrational Schrödinger equation, J being the rotational quantum number. In equation (56),

$$\rho(J) = \left[g_J(2J+1)\exp\left(\frac{-(E_{0,J}-E_{0,0})}{kT}\right)\right] \Bigg/ \left[\sum_J g_J(2J+1)\exp\left(\frac{-(E_{0,J}-E_{0,0})}{kT}\right)\right]. \quad (57)$$

Here $E_{0,J}$ is the rovibrational energy and g_J is the nuclear spin degeneracy factor.

The formula for the pure vibrational contribution to the hypermagnetizabilities η of diamagnetic molecules, obtained as described in detail in [57, 59] (see also [109]) is:

$$\eta^{\upsilon}_{\alpha\beta,\gamma\delta} = \frac{2}{\hbar}\sum_{n\neq g}\frac{[(\mu_\alpha)_{ng}(\xi_{\gamma\delta,\beta})_{ng} + (\mu_\beta)_{ng}(\xi_{\gamma\delta,\alpha})_{ng} + (\alpha_{\alpha\beta})_{ng}(\chi_{\gamma\delta})_{ng}]}{\omega_n}$$
$$+\frac{2}{\hbar^2}\sum_{m\neq g}\sum_{n\neq g}\frac{[(\mu_\alpha)_{gm}(\bar{\chi}_{\gamma\delta})_{mn}(\mu_\beta)_{ng} + (\mu_\alpha)_{gm}(\bar{\mu}_\beta)_{mn}(\chi_{\gamma\delta})_{ng} + (\mu_\beta)_{gm}(\bar{\mu}_\alpha)_{mn}(\chi_{\gamma\delta})_{ng}]}{\omega_n\,\omega_m}. \quad (58)$$

$(X)_{mn}$ denotes here the vibrational transition moment between the m and n vibrational states for the property X, that is $(X)_{mn} = \langle\upsilon(m)|X|\upsilon(n)\rangle$, while $\hbar\omega_n$ is the vibrational transition energy. For homonuclear diatomics, with no permanent electric or magnetic dipole moment,

$$\eta^{\upsilon}_{\alpha\beta,\gamma\delta} = \frac{2}{\hbar}\sum_{n\neq g}\frac{(\alpha_{\alpha\beta})_{ng}(\chi_{\gamma\delta})_{ng}}{\omega_n} \quad (59)$$

and, for the hypermagnetizability anisotropy, one obtains [48, 50]

$$\Delta\eta^{\upsilon} = \frac{4}{15\hbar}\sum_{n\neq g}\frac{(\Delta\alpha)_{ng}(\Delta\chi)_{ng}}{\omega_n}. \quad (60)$$

The vibrational contribution to the CME of some molecular systems have been estimated by Fowler and Buckingham [48] (H_2), by Bishop *et al.* [50] (H_2 and D_2) and by Cybulski and Bishop [57] (H_2, N_2, HF and CO), always within the BO approximation. Bishop *et al.* [50] suggested that the effects of the breakdown of the BO approximation on the hypermagnetizability anisotrophy of H_2 and D_2 would be negligible. Spin–orbit and intermolecular interactions have been neglected in all theoretical treatments of CME so far. It should also be noted that the $\Delta\alpha$ and $\Delta\chi$ terms in equation (30) should be zero-point vibrationally averaged as well as include any pure vibrational contributions, as will be the case for polar and/or paramagnetic molecules.

In general and in finite basis set calculations with a standard gauge-dependent approach, both the paramagnetic and diamagnetic contributions to the magnetizability χ and to the hypermagnetizability η depend on the choice of magnetic induction origin R_G which enters equations (44) and (45). Gauge-independent results can be obtained provided that certain constraints (sum rules) are satisfied, as discussed in [57, 110, 111]. Cybulski and Bishop [57] showed how, for homonuclear diatomic molecules, the diamagnetic contribution (η^{d}) to the hypermagnetizability is magnetic gauge origin independent while, for heteronuclear diatomics, η^{d} depends linearly on the change in gauge origin. The dependence of η^{p} is slightly more complicated. Magnetic gauge origin independence of the results is guaranteed [112] by the use in the calculations of explicit-perturbation (magnetic-field)-dependent basis sets, as, for instance, the London atomic orbitals (LAOs) or gauge-invariant atomic orbitals (GIAOs) [113–115]. By employing LAO, gauge-origin-independent basis-set-limit results for magnetizabilities and hypermagnetizabilities can be obtained with the use of relatively small basis sets [60, 64, 65]. The very recent application of the continuous transformation of origin of current density approach to the analytical determination of gauge-origin-independent hypermagnetizabilities, although currently limited to first-order electric field perturbed magnetizabilities, should be mentioned for its possible potential [116].

Recent developments in theoretical and computational methods have enabled *ab initio* studies of a wide variety of atomic and molecular electric, magnetic and optical properties to be undertaken [66]. Thus *ab initio* calculated values not only of $\Delta\alpha$ and $\Delta\chi$ but also of $\Delta\eta$ for some gases are available at different levels of accuracy. The main difficulties arise in the calculation of $\Delta\eta$, whose importance in the description of the CME increases as the spherical character of the system increases (i.e. the symmetry of the system becomes higher). There are only a few electron-correlated calculations of the hypermagnetizability anisotropy in atoms and small molecules. For most systems, calculations have been restricted to the self-consistent field (SCF) approximation. Electron correlation plays an important role in the description of the high-order magnetic properties involved in the CME. Apart from the results obtained by Bishop and co-workers [50, 52] for the frequency-dependent hypermagnetizabilities of H_2 (D_2) and helium with explicitly electron-correlated wavefunctions (ECWs), the approximations employed to compute correlated hypermagnetizability anisotropies $\Delta\eta$ are the second-order Møller–Plesset (MP2) theory (H_2, N_2, HF, CO [57], He, Ne, Ar [56]) or the multiconfigurational self-consistent field (MCSCF) response theory (neon [54], argon [58], N_2, C_2H_2, HCN, H_2O [60], CO, CH_4 [64] and C_2H_4 [65]). Very recently third-order Møller–Plesset (MP3) and linearized coupled clusters (doubles) theories have been applied to H_2, N_2, HF and CO [62]. In [57], frequency-dependent molecular hypermagnetizabilities were computed, as second derivatives of the electric dipole dynamic polarizability with respect to a static magnetic field. A mixed analytical–numerical finite-magnetic-field approach was employed. A finite-electric-field technique, which cannot be used to obtain frequency-dependent hypermagnetizabilities, was used in [60, 64, 65].

There are some discrepancies between the values computed for the same quantity by different authors. In the case of helium, the value of $\Delta\eta$ from [55] and from [52], both at the correlated level, differ by about 3%, and in this case one would expect that most of the discrepancy arises from the difference between the MP2 approach and the more exact explicitly electron-correlated approach. For larger systems the choice between essentially equivalent approaches is much less obvious; see, for instance, neon [54, 56] and argon [56, 58]. When comparing theoretical and experimental values, one should realize that both carry error bars. In [54] the error on $\Delta\eta$ for neon was evaluated to be of the order of about 5%. On the other hand, often these uncertainties are smaller than those accompanying the published experimental values. As an example, the experimental value for the CME of helium published in [30] has a 20% error bar.

4. Definitions and units

Different definitions and units can be found in the literature for the quantities discussed here, and a short section on notation and conventions seems to be appropriate. Our references for this section are the 'green book' edited by Mills *et al.* [117] and the review by Cohen and Taylor [118]. Some experimentalists employ a Cotton–Mouton constant C_{CM} defined [14] through the equation

$$\Delta n = \lambda C_{\mathrm{CM}} B^2. \tag{61}$$

C_{CM} is usually given in emu units, that is $\mathrm{G}^{-2}\ \mathrm{cm}^{-1}$.

Theoreticians usually refer to the Buckingham and Pople ${}_{\mathrm{m}}C$ molar constant [6] which is defined in equation (27). In [6, 12], ${}_{\mathrm{m}}C$ was given in emu units of $\mathrm{cm^3\,G^{-2}\,mol^{-1}}$, or more correctly $\mathrm{cm^3\,G^{-2}\,mol^{-1}}\,(4\pi\varepsilon_0)$. Elsewhere [19, 21, 22, 26–28, 31–33] a definition of ${}_{\mathrm{m}}C$ is referred to equation (27) for a refractive index n of the unperturbed medium such that $n-1 \approx 0$. The two definitions are formally different when $n-1 \neq 0$. The SI units $\mathrm{m^5A^{-2}\,mol^{-1}}$ are also often used for ${}_{\mathrm{m}}C$.† The appendix in [20] and a specific section on units in [21] discuss in some detail the relationships between emu and SI units employed in CME. König [7] introduced a different definition of the molar Cotton–Mouton constant, indicated here as ${}_{\mathrm{m}}C'$, for the case of refractive index n of the unperturbed medium such that $n-1 \approx 0$, that is

$$\Delta n = \frac{3B^2}{2V_{\mathrm{m}}(4\pi\varepsilon_0)}\,{}_{\mathrm{m}}C'. \tag{62}$$

${}_{\mathrm{m}}C'$ is given in units of $\mathrm{cm^3\,G^{-2}\,mol^{-1}}$ in [15–17, 20, 25] and units of $\mathrm{m^3\,T^{-2}\,mol^{-1}}$ in [13]. It is straightforward to see that

$${}_{\mathrm{m}}C' = 9\,{}_{\mathrm{m}}C. \tag{63}$$

The formulae linking C_{CM} and ${}_{\mathrm{m}}C$ are (with the temperature in kelvins, and the wavelengths in centimetres)

$$C_{\mathrm{CM}}\,(\mathrm{G^{-2}\,cm^{-1}}) = \frac{0{\cdot}164\,518}{\lambda T}\,{}_{\mathrm{m}}C\,(\mathrm{cm^3\,G^{-2}\,mol^{-1}}\,(4\pi\varepsilon_0)), \tag{64 a}$$

$$C_{\mathrm{CM}}\,(\mathrm{G^{-2}\,cm^{-1}}) = \frac{0{\cdot}164\,518\times 10^{-2}}{\lambda T}\,{}_{\mathrm{m}}C\,(\mathrm{m^3\,T^{-2}\,mol^{-1}}\,(4\pi\varepsilon_0)), \tag{64 b}$$

$$C_{\mathrm{CM}}\,(\mathrm{G^{-2}\,cm^{-1}}) = \frac{1{\cdot}041\,82\times 10^{9}}{\lambda T}\,{}_{\mathrm{m}}C\,(\mathrm{m^5\,A^{-2}\,mol^{-1}}). \tag{64 c}$$

To introduce explicitly the temperature T we have assumed a pressure P of 1 atm and ideal-gas behaviour. As seen above for Δn, the Cotton–Mouton constant depends linearly on the pressure.

In the next section we report and discuss (where possible) only the value of Δn, which is, by definition, dimensionless. When comparing different results we always refer to Δn given at $B = 1$ T and $P = 1$ atm. We label this reference as Δn_{u}. The relation between Δn and Δn_{u} is

$$\Delta n(P = 1\ \mathrm{atm}) = \Delta n_{\mathrm{u}}\left(\frac{B(\mathrm{T})}{1\ \mathrm{T}}\right)^2 = \Delta n_{\mathrm{u}}\left(\frac{B(\mathrm{G})}{10^4\ \mathrm{G}}\right)^2 = \Delta n_{\mathrm{u}}\left(\frac{B\,(\mathrm{au})}{4{\cdot}254\,38\times 10^{-6}\ \mathrm{au}}\right)^2. \tag{65}$$

The relationships between Δn_{u} and the Cotton–Mouton constants introduced before are

$$\Delta n_{\mathrm{u}} = \lambda \times 10^8\, C_{\mathrm{CM}}\,(\mathrm{G^{-2}\,cm^{-1}}), \tag{66 a}$$

$$\Delta n_{\mathrm{u}} = \frac{1{\cdot}645\,18\times 10^{7}}{T}\,{}_{\mathrm{m}}C\,(\mathrm{cm^3\,G^{-2}\,mol^{-1}}\,(4\pi\varepsilon_0)), \tag{66 b}$$

$$\Delta n_{\mathrm{u}} = \frac{1{\cdot}041\,82\times 10^{17}}{T}\,{}_{\mathrm{m}}C\,(\mathrm{m^5\,A^{-2}\,mol^{-1}}). \tag{66 c}$$

---

† The use of these units is incorrect and should be discouraged, since they are based on the use of the magnetic field H (whose SI unit is $\mathrm{A\ m^{-1}}$) rather than of the magnetic flux density B (SI unit T).

The microscopic properties $\Delta\eta$, $\Delta\alpha$ and $\Delta\chi$ are usually given by theoreticians in atomic units (au) (often called 'natural' units) [119]. From equation (34), the following relation holds for axial molecules between Δn_u and $\Delta\eta$, $\Delta\alpha$, $\Delta\chi$ given in atomic units:

$$\Delta n_u = \frac{6{\cdot}183\,81 \times 10^{-14}}{T}\left(\Delta\eta + \frac{4{\cdot}210\,31 \times 10^{4}}{T}\Delta\alpha\,\Delta\chi\right). \tag{67}$$

To end this section, we give the conversion factors from atomic units to certain other units:

1 au of $\alpha = e^2 a_0^2 E_h^{-1} \approx 1{\cdot}648\,78 \times 10^{-41}\ \mathrm{C^2\,m^2\,J^{-1}} \approx 1{\cdot}481\,85 \times 10^{-25}\ (4\pi\varepsilon_0)\ \mathrm{cm^3}$.
1 au of $\chi = e^2 a_0^2 m_e^{-1} \approx 7{\cdot}891\,04 \times 10^{-29}\ \mathrm{J\,T^{-2}} \approx 7{\cdot}891\,04 \times 10^{-30}\ \mathrm{erg\,G^{-2}}$.
1 au of $\eta = e^4 a_0^4 m_e^{-1} E_h^{-2} \approx 2{\cdot}984\,25 \times 10^{-52}\ \mathrm{C^2\,m^2\,J^{-1}\,T^{-2}} \approx 2{\cdot}682\,11 \times 10^{-44}\ (4\pi\varepsilon_0)\ \mathrm{cm^3\,G^{-2}}$.
1 au of $E = E_h e^{-1} a_0^{-1} \approx 5{\cdot}142\,21 \times 10^{11}\ \mathrm{V\,m^{-1}} \approx 1{\cdot}715\,26 \times 10^{7}\ \mathrm{Fr\,cm^{-2}}\,(4\pi\varepsilon_0)^{-1}$.
1 au of $B = \hbar e^{-1} a_0^{-2} \approx 2{\cdot}350\,52 \times 10^{5}\ \mathrm{T} \approx 2{\cdot}350\,52 \times 10^{9}\ \mathrm{G}$.

5. Review of published data

In tables 2–5 the values of Δn_u extracted from the experimental data found in the literature for gases are given. We began our search from the 1967 paper of Buckingham *et al.* [6] and restricted it to international journals.

In some cases, experimentalists have derived values for the microscopic properties from measurements of the Cotton-Mouton constant, that is from measurements of Δn. In order to be able to do this, one has to make some assumptions. For example in the case of molecules, from the values of Δn as function of temperature, one could in principle obtain $\Delta\eta$ and a value for the product $\Delta\alpha\,\Delta\chi$. To get the value of $\Delta\chi$, one has to assume a value for $\Delta\alpha$ or vice versa. Usually the unknown value must come from a different type of measurement. If the value of Δn has been measured at only one temperature, to extract a value for one of the three microscopic properties, the other two must be estimated independently. In the case of atoms, since Δn depends on only $\Delta\eta$, the connection between macroscopic and microscopic properties is straightforward. In tables 2–5 we report only values of the quantity Δn_u. An analysis of the different assumptions made to extract $\Delta\eta$, $\Delta\alpha$ or $\Delta\chi$ is beyond the scope of this review.

For simplicity, when measurements were done at different temperatures, only the result at the temperature nearest to room temperature (293·15 K) is listed. The reader should refer to the original paper for further information. Where the experimental value has an error larger than 50% of its value, we refer to it as a limit, meaning that its statistical significance is so poor that the result can only be used as an upper limit for the physical effect. This criterion was not applied to the data on SF_6 taken from [6] since it is the only existing value of the property for this gas.

In table 6 we collect the values of $\Delta\eta$ and Δn_u resulting from theory for atoms and in table 7 the values of $\Delta\alpha$, $\Delta\chi$ and $\Delta\eta$ for molecules. With the development of powerful computational techniques in the past few years, quantum chemists can now compute $\Delta\alpha$ and $\Delta\chi$ quite easily and, with more difficulty, $\Delta\eta$. Recovering Δn_u is straightforward in the case of atoms; see equations (31) and (65). In the case of molecules, on the other hand, theoreticians do not usually give the value of the physically measurable property Δn but report the separate values of the microscopic properties. Only in a few cases are all three properties included. In preparing table 7 we had to decide whether to include only data taken from these sources or to extend the list to other systems, for which the values of the anisotropies are available from different sources. We decided

Table 2. Experimental values of Δn_u for inorganic species.

Species	Formula	Reference	λ (Å)	T (K)	Δn_u	T range (K)
Helium[a]	He	30[b]	5145	273·15	$(1{\cdot}80 \pm 0{\cdot}36) \times 10^{-16}$[c]	
Neon[d]	Ne	29[e]	5145	298·15	$(2{\cdot}83 \pm 0.15) \times 10^{-16}$	
Argon[f]	Ar	18[g]	5145	273·15	$(6{\cdot}8 \pm 1{\cdot}0) \times 10^{-15}$[h]	
Krypton[i]	Kr	18	5145	273·15	$(9{\cdot}9 \pm 1{\cdot}1) \times 10^{-15}$[h]	
Xenon[k]	Xe	18	5145	273·15	$(2{\cdot}29 \pm 0{\cdot}10) \times 10^{-14}$[h]	
Hydrogen	H_2	23[g]	5145	273·15	$(8{\cdot}28 \pm 0.57) \times 10^{-15}$[j]	
		25	6328	286	$(8.82 \pm 0.25) \times 10^{-15}$	187–402
Deuterium	D_2	23[g]	5145	273·15	$(7.25 \pm 0{\cdot}72) \times 10^{-15}$[j]	
		25	6328	285	$(10{\cdot}04 \pm 0{\cdot}75) \times 10^{-15}$	285–369
Carbon monoxide	CO	6	5461	293·15	$(-2{\cdot}24 \pm 0{\cdot}45) \times 10^{-13}$	
		17	6328	294·15	$(-1{\cdot}90 \pm 0{\cdot}12) \times 10^{-13}$	203–393
		11[l]	6328	293·15	$(-1{\cdot}80 \pm 0{\cdot}06) \times 10^{-13}$	
Nitrogen	N_2	6	5461	293·15	$(-2{\cdot}47 \pm 0{\cdot}17) \times 10^{-13}$	
		11[l]	6328	293·15	$(-2{\cdot}37 \pm 0{\cdot}12) \times 10^{-13}$	
		13	6328	293·15	$(-3{\cdot}06 \pm 0{\cdot}42) \times 10^{-13}$	
		14	5145	290·15	$(-2{\cdot}56 \pm 0{\cdot}13) \times 10^{-13}$	
		16	6328	293·15	$(-2{\cdot}62 \pm 0{\cdot}08) \times 10^{-13}$	203–393
		17	6328	294·15	$(-2{\cdot}43 \pm 0{\cdot}12) \times 10^{-13}$	203–393
		29	5145	298·15	$(-2{\cdot}26 \pm 0{\cdot}10) \times 10^{-13}$	

[a] Also see the experimental estimate cited in [52] as a private communication from W. Hüttner: Δn_u (He) = $(+2{\cdot}5 \pm 2{\cdot}5) \times 10^{-16}$ at 273·15 K and λ = 6238 Å.

[b] Limits can also be found in [6, 18].

[c] Given relative to N_2 but measured at different temperatures; Δn_u (N_2) assumed equal to $-2{\cdot}26 \times 10^{-13}$ at 298·15 K; the authors scale the two gases differently with temperature.

[d] Also see the experimental estimate cited in [52] as a private communication from W. Hüttner: Δn_u (Ne) = $(+9{\cdot}3 \pm 6{\cdot}8) \times 10^{-16}$ at 273·15 K and λ = 6238 Å.

[e] Limits can be also found in [18].

[f] Also see the experimental estimate cited in [52] as a private communication from W. Hüttner: Δn_u (Ar) = $(+5{\cdot}9 \pm 0{\cdot}3) \times 10^{-15}$ at 273·15 K and λ = 6238 Å.

[g] Limits can also be found in [6].

[h] Measured at room temperature and relative to N_2, assuming that Δn_u (N_2) = $-2{\cdot}62 \times 10^{-13}$ at 273·15 K.

[i] Also see the experimental estimate cited in [52] as a private communication from W. Hüttner: Δn_u (Kr) = $(+10{\cdot}2 \pm 0{\cdot}7) \times 10^{-15}$ at 273·15 K and λ = 6238 Å.

[k] Also see the experimental estimate cited in [52] as a private communication from W. Hüttner: Δn_u (Xe) = $(+24{\cdot}1 \pm 1{\cdot}2) \times 10^{-15}$ at 273·15 K and λ = 6238 Å.

[j] Measured at room temperature and relative to N_2, assuming Δn_u (N_2) = $-2{\cdot}7 \times 10^{-13}$ at 273·15 K.

[l] As reported in [17].

on this last option. We selected all systems for which *ab initio* estimates of $\Delta\eta$ were published, and associated with these estimates the values of $\Delta\alpha$ and $\Delta\chi$ provided by the same or different workers. We believe that, even if the data might come from different workers and different techniques (meaning different levels of accuracy), all together they furnish reliable reference values for the physical quantity and can be of help to the experimentalist. We list, in most cases, correlated results, and only when these are not yet available will the reader find SCF estimates.

Some of the *ab initio* results for the anisotropies in table 7 include the vibrational contributions, as discussed above. The vibrational corrections to the electronic properties may in some cases be non-negligible and should be taken into account when comparing theory and experiment.

Table 3. Experimental values of Δn_u for inorganic molecules.

Molecule	Formula	Reference	λ (Å)	T (K)	Δn_u	T range (K)
Nitrogen monoxide	NO	20	6328	293·15	$(2\cdot08 \pm 0\cdot02) \times 10^{-11}$	188–393
Oxygen	O_2	14	5145	290·15	$(-2\cdot52 \pm 0\cdot06) \times 10^{-12}$	
		16	6328	294	$(-2\cdot52 \pm 0\cdot06) \times 10^{-12}$	200–400[a]
		28	6328	298.6	$(-2\cdot56 \pm 0\cdot04) \times 10^{-12}$	298·6–463·7
Carbon dioxide	CO_2	6	5461	293·15	$(-5\cdot61 \pm 0\cdot28) \times 10^{-13}$	
		11[b]	6328	293·15	$(-5\cdot61 \pm 0\cdot25) \times 10^{-13}$	
		13	6328	293·15	$(-5\cdot90 \pm 0\cdot94) \times 10^{-13}$	
		17	6328	294·15	$(-5\cdot90 \pm 0\cdot12) \times 10^{-13}$	203–393
Carbon disulphide	CS_2	17	6328	294·15	$(-7\cdot83 \pm 0\cdot12) \times 10^{-12}$	203–393
		11[b]	6328	293·15	$(-7\cdot17 \pm 0\cdot12) \times 10^{-12}$	
Carbonyl sulphide	OCS	13	6328	293·15	$(-1\cdot77 \pm 0\cdot21) \times 10^{-12}$	
		17	6328	294·15	$(-1\cdot81 \pm 0\cdot03) \times 10^{-12}$	203–393
		11[b]	6328	293·15	$(-1\cdot61 \pm 0\cdot06) \times 10^{-12}$	
Dinitrogen monoxide	N_2O	6	5461	293·15	$(-1\cdot46 \pm 0\cdot03) \times 10^{-12}$	
		13	6328	293·15	$(-1\cdot32 \pm 0\cdot18) \times 10^{-12}$	
		17	6328	294·15	$(-1\cdot37 \pm 0\cdot03) \times 10^{-12}$	203–393
		11[b]	6328	293·15	$(-1\cdot27 \pm 0\cdot02) \times 10^{-12}$	
Sulphur hexafluoride	SF_6	6	5461	293·15	$(-7\cdot9 \pm 4\cdot5) \times 10^{-14}$	

[a] Also measured at liquid-nitrogen temperature.

[b] As reported in [17].

Table 4. Experimental values of Δn_u for organic molecules.

Molecule	Formula	Reference	λ (Å)	T (K)	Δn_u	T range (K)
Methane[a]	CH_4	26[b]	6328	294·4	$(1.59 \pm 0\cdot21) \times 10^{-14}$	
Acetylene	C_2H_2	15	6328	293·15	$(-2\cdot03 \pm 0\cdot11) \times 10^{-13}$	193–393
		33	6328	293·1	$(-1\cdot98 \pm 0\cdot08) \times 10^{-13}$	293·1–442·2
Ethylene	C_2H_4	6	5461	293·15	$(2\cdot47 \pm 0\cdot24) \times 10^{-13}$	
		11[c]	6328	293·15	$(2\cdot96 \pm 0\cdot22) \times 10^{-13}$	
		15	6328	293·15	$(3\cdot13 \pm 0\cdot06) \times 10^{-13}$	193–393
Ethane	C_2H_6	6	5461	293·15	$(-7\cdot86 \pm 2\cdot24) \times 10^{-14}$	
		11[c]	6328	293·15	$(-1\cdot20 \pm 0\cdot11) \times 10^{-13}$	
		15	6328	293·15	$(-1\cdot48 \pm 0\cdot09) \times 10^{-13}$	193–394
Methyl fluoride	CH_3F	31	6328	296·1	$(-6\cdot97 \pm 0\cdot21) \times 10^{-13}$	296·1, 296·2
Propine	C_3H_4	13	6328	293·15	$(-1\cdot15 \pm 0\cdot16) \times 10^{-12}$	
Oxirane	C_2H_4O	32	6328	293·6	$(3\cdot20 \pm 0\cdot25) \times 10^{-13}$	292·7–447·6
Dimethyl ether	C_2H_6O	32	6328	294·9	$(-2\cdot93 \pm 0\cdot04) \times 10^{-13}$	294·9–414·5
Methyl chloride	CH_3Cl	26[d]	6328	294·6	$(-5\cdot34 \pm 0\cdot07) \times 10^{-13}$	252·0–407·6
Isobutane	C_4H_{10}	13	6328	293·15	$(-1\cdot3 \pm 0\cdot8) \times 10^{-13}$	
Dimethyl sulphide	C_2H_6S	32	6328	293·2	$(-4\cdot96 \pm 0\cdot45) \times 10^{-13}$	293·2–443·9
Furan	C_4H_4O	32	6328	294·6	$(5\cdot27 \pm 0\cdot01) \times 10^{-12}$	294·6–445·0

[a] Also see the experimental estimate cited in [52] as a private communication from W. Hüttner: Δn_u (CH_4) = $(+1\cdot09 \pm 0\cdot07) \times 10^{-14}$ at 273·15 K and λ = 6238 Å.

[b] Limits can also be found in [6].

[c] As reported in [15].

[d] Limits can also be found in [31].

Table 5. Experimental values of Δn_u for organic molecules.

Molecule	Formula	Reference	λ (Å)	T (K)	Δn_u	T range (K)
Cyclopropane	C_5H_{10}	6	5461	293·15	$(6{\cdot}5 \pm 1{\cdot}4) \times 10^{-13}$	
		21	6328	295·5	$(3{\cdot}31 \pm 0{\cdot}05) \times 10^{-13}$	261·4–404·3
Benzene	C_6H_6	12	6328	293·15	$(1{\cdot}29 \pm 0{\cdot}06) \times 10^{-11}$	
		13	6328	293	$(1{\cdot}51 \pm 0{\cdot}04) \times 10^{-11}$	
		19	4416	300·1	$(1{\cdot}50 \pm 0{\cdot}04) \times 10^{-11}$	300·1–455·5
Thiophene	C_4H_4S	32	6328	294·1	$(9{\cdot}95 \pm 0{\cdot}14) \times 10^{-12}$	294·1–446·0
Cyclohexane	C_6H_{12}	27	4416	400·2	$(-4{\cdot}63 \pm 0{\cdot}26) \times 10^{-13}$	
Methyl bromide	CH_3Br	31	6328	294·2	$(-6{\cdot}94 \pm 0{\cdot}18) \times 10^{-14}$	294·2–421·7
Fluorobenzene	C_6H_5F	22	4416	403·9	$(7{\cdot}84 \pm 0{\cdot}16) \times 10^{-12}$	
		22	6328	405·6	$(7{\cdot}45 \pm 0{\cdot}15) \times 10^{-12}$	
Chloroform	$CHCl_3$	26	6328	319	$(-1{\cdot}13 \pm 0{\cdot}05) \times 10^{-12}$	319·0–471·2
1,3,5-Trifluorobenzene	$C_6H_3F_3$	12	6328	293·15	$(1{\cdot}00 \pm 0{\cdot}04) \times 10^{-11}$	
		19	4416	303·8	$(1{\cdot}08 \pm 0{\cdot}03) \times 10^{-11}$	303·8–455·5
Methyl iodide	CH_3I	31	6328	295·3	$(-1{\cdot}10 \pm 0{\cdot}04) \times 10^{-12}$	295·3–466·8
Carbon tetrachloride	CCl_4	26	6328	396·6	$(7{\cdot}9 \pm 2{\cdot}4) \times 10^{-14}$	
Hexafluorobenzene	C_6F_6	12	6328	293·15	$(8{\cdot}81 \pm 0{\cdot}38) \times 10^{-12}$	
		19	4416	304·1	$(10{\cdot}11 \pm 0{\cdot}17) \times 10^{-12}$	304·1–453·3

Table 6. Theoretical values of $\Delta\eta$ and Δn_u (at $T = 273{\cdot}15$ K) for atoms and atomic ions.

Species	Symbol	Reference	Method	λ (A)	$\Delta\eta$ (au)	Δn_u
Hydrogen	H	45, 48	Exact	∞	13·33	$3{\cdot}0178 \times 10^{-15}$
Helium	He	52	ECW[a]	∞	1·06061	$2{\cdot}40113 \times 10^{-16}$
		52	ECW[a]	6328	1·05791[b]	$2{\cdot}39501 \times 10^{-16}$
		55	MP2[c]	5145	1·0287	$2{\cdot}3288 \times 10^{-16}$
		51	ECW[d]	∞	1·06	$2{\cdot}40 \times 10^{-16}$
Neon	Ne	54	MCSCF[e]	5145	2·670	$6{\cdot}04 \times 10^{-16}$
		55	MP2[c]	5145	3·034	$6{\cdot}869 \times 10^{-16}$
		55	MP2[c]	6328	3·029	$6{\cdot}858 \times 10^{-16}$
Argon	Ar	58	MCSCF[e]	5145	24·14	$5{\cdot}465 \times 10^{-15}$
		55	MP2[c]	5145	25·70	$5{\cdot}818 \times 10^{-15}$
		55	MP2[c]	6328	25·68	$5{\cdot}814 \times 10^{-15}$
Krypton	Kr	56	SCF[f]	∞	48·61	$1{\cdot}101 \times 10^{-14}$
Xenon	Xe	56	SCF[f]	∞	117·7	$2{\cdot}665 \times 10^{-14}$
Hydride anion	H^-	63	SCF[g]	∞	352·6	$7{\cdot}982 \times 10^{-14}$
Lithium cation	Li^+	51	SCF[h]	∞	0·016077	$3{\cdot}6396 \times 10^{-18}$
		63	SCF[g]	∞	0·01548	$3{\cdot}5045 \times 10^{-18}$
Fluoride anion	F^-	63	SCF[g]	∞	67·33	$1{\cdot}524 \times 10^{-14}$
Sodium cation	Na^+	63	SCF[g]	∞	0·4919	$1{\cdot}114 \times 10^{-16}$
Chloride anion	Cl^-	63	SCF[g]	∞	331·1	$7{\cdot}496 \times 10^{-14}$
Potassium cation	K^+	63	SCF[g]	∞	6·631	$1{\cdot}501 \times 10^{-15}$

[a] Explicitly ECW.

[b] Slightly revised with respect to the value given in [52].

[c] MP2 perturbation theory and finite magnetic field.

[d] Estimated by extracting the paramagnetic contribution from the electron correlated dipole polarizabilities computed in [120] and the diamagnetic contribution from the electron-correlated dipole–dipole–quadrupole polarizabilities of [84].

[e] MCSCF quadratic response.

[f] SCF and finite electric field.

[g] SCF cubic response.

[h] Time-dependent Hartree–Fock perturbation theory.

Table 7. Theoretical values of $\Delta\alpha$, $\Delta\chi$ and $\Delta\eta$ for molecules[a].

Molecule	Formula	Ref.	Method	$\Delta\alpha$ (au)	Ref.	Method	$\Delta\chi$ (au)	Ref.	Method	λ (Å)	$\Delta\eta$ (au)
Hydrogen	H_2	59	MP2[b]	2·069[c]	57	MP2[b]	0·1114[c]	50	ECW[d]	∞	10·806[e]
		83[f]	ECW[d]	1·808 882	122	ECW[d]	0·1124[c]	50	ECW[d]	6328	10·547[e]
		123	ECW[d]	2·0228[c]				50	ECW[d]	5145	10·386[e]
Deuterium	D_2	123	ECW[d]	1·9605[c]	122	ECW[d]	0·1100[c]	50	ECW[d]	∞	10·571[e]
								50	ECW[d]	6328	10·374[e]
								50	ECW[d]	5145	10·175[e]
Methane	CH_4		Exact	0		Exact	0	52	Semiempirical[g]	∞	41·8
								64[h]	MCSCF–GIAO[i]	∞	40·65
Ammonia	NH_3	126	CCSD(T)[j]	2·01	127	MCSCF–IGLO[k]	0·23	61	SCF[l]	∞	23·97
Water[m]	H_2O	60	MCSCF–GIAO[n]	0·44, 0·79, 0·36[o]	60[q]	MCSCF–GIAO[n]	0·049, 0·042 −0·007[p]	60[q]	MCSCF–GIAO[i]	∞	32·06
		126	CCSD(T)[j]	0·3804, 0·2881 −0·0923[o]	110	MP2[b]	0·049, 0·041, −0·008[p]				
		128	MP4[r]	0·37, 0·2, −0·17[o]	129	MCSCF–GIAO[n]	0·0498, 0·0417, −0·0081[p]				
Hydrogen fluoride	HF	59	MP2[b]	1·227[c]	57	MP2[b]	0·107[c]	57	MP2[s]	∞	10·32[t]
		126[f]	CCSD(T)[j]	1·10	129	MCSCF–GIAO[n]	0·107	57	MP2[s]	6328	10·26[u]
					127	MCSCF–IGLO[k]	0·103	57	MP2[s]	5145	10·22[v]
Acetylene	C_2H_2	60	MCSCF–GIAO[n]	11·29	60	MCSCF–GIAO[n]	−0·41	60[w]	MCSCF–GIAO[i]	∞	86·85
		130	CCD[x]	11·58							
Hydrogen cyanide	HCN	60	MCSCF–GIAO[n]	8·14	60	MCSCF–GIAO[n]	−1·15	60[y]	MCSCF–GIAO[i]	∞	41·40
		131	CCSD(T)[l]	8·85[z]	110	MP2[b]	−1·252				
Nitrogen	N_2	60	MCSCF–GIAO[n]	4·37	60	MCSCF–GIAO[n]	−1·71	60[aa]	MCSCF–GIAO[i]	∞	27·94
		59	MP2[b]	4·22[c]	57	MP2[b]	−1·705[c]	57	MP2[s]	∞	22·18[bb]
		126	CCSD(T)[j]	4·869	129	MCSCF–GIAO[n]	−1·722	57	MP2[s]	6328	22·55[cc]
					127	MCSCF–IGLO[k]	−1·665	57	MP2[s]	5145	22·74[dd]
Carbon monoxide	CO	59	MP2[b]	3·76[c]	57	MP2[b]	−1·649[c]	57	MP2[s]	∞	36·05[ee]
		126	CCSD(T)[j]	3·92	129	MCSCF–GIAO[n]	−1·605	57	MP2[s]	6328	37·54[ff]
		64	MCSCF–GIAO[n]	3·605	64	MCSCF–GIAO[n]	−1·668	57	MP2[s]	5145	38·34[gg]
					127	MCSCF–IGLO[k]	−1·597	64[hh]	MCSCF–GIAO[i]	∞	35·41
Ethylene	C_2H_4	65	MCSCF–GIAO[n]	2·33, −9·06, −11·40[o]	65	MCSCF–GIAO[n]	1·99, 0·64, −1·36[p]	65	MCSCF–GIAO[i]	∞	61·0[ii]
		126	CCSD(T)[j]	2·909, −8·706, −11·615[o]							
Benzene	C_6H_6	53	SCF	−35·58	53	SCF	$-544{\cdot}53\times10^{-3}$	53	SCF	∞	0·04433
		132	SCF[jj]	−32·5	132	SCF[kk]	$-781{\cdot}749\times10^{-3}$				

[a] Static electric polarizability and magnetizability anisotropies ($\lambda = \infty$).

[b] MP2 perturbation theory.

[c] Vibrationally averaged.

[d] Explicitly ECW.

[e] Includes all vibrational effects.

[f] For a comprehensive collection of other accurate values see [121].

[g] ‘Spherical molecule’ approximation. Estimated from an experimentally derived sum rule [124] and calculated dipole–dipole–quadrupole polarizability [125].

[h] Coriani *et al.* give a value of the molar Cotton–Mouton constant corresponding to $\Delta n_u = 9{\cdot}2 \times 10^{-15}$ at 273·15 K.

[i] MCSCF linear response and finite field. GIAOs employed for gauge-invariant magnetic properties.

[j] Coupled clusters singles doubles (triples) (CCSD(T)).

[k] MCSCF and individual gauge localized orbitals (IGLOs).

[l] SCF cubic response theory.

[m] In this case, equation (67) can be written (with the temperatures in kelvins and the anisotropies in atomic units) as in [60]: $\Delta n_u = 6{\cdot}18381 \times 10^{-14} T^{-1}\{\Delta\eta + 2{\cdot}10515 \times 10^4 T^{-1}(\Delta\alpha_{xx,yy}\Delta\chi_{xx,yy} + \Delta\alpha_{yy,zz}\Delta\chi_{yy,zz} + \Delta\alpha_{xx,zz}\Delta\chi_{xx,zz})\}$ with $\Delta\alpha_{ii,jj} = \alpha_{ii} - \alpha_{jj}$ and $\Delta\chi_{ii,jj} = \chi_{ii} - \chi_{jj}$.

[n] MCSCF linear response. GIAOs employed for gauge-invariant magnetic properties.

[o] $\Delta\alpha_{xx,yy}$, $\Delta\alpha_{xx,zz}$, $\Delta\alpha_{yy,zz}$.

[p] $\Delta\chi_{xx,yy}$, $\Delta\chi_{xx,zz}$, $\Delta\chi_{yy,zz}$.

[q] The authors give a value of the molar Cotton–Mouton constant corresponding to $\Delta n_u = 8{\cdot}4 \times 10^{-15}$ at 273·15 K.

[r] Møller–Plesset fourth-order (MP4) perturbation theory.

[s] MP2 perturbation theory and finite magnetic field.

[t] Includes the vibrational contribution; see equation (32) in [57]. Electronic contribution is 10·01 au. See also the MP3 perturbation theory (8·22 au) and the linearized coupled clusters doubles (L-CCD) (8·57 au) estimates of the electronic contribution in [62].

[u] Includes the vibrational contribution; see equation (32) in [57]. The electronic contribution is 9·95 au.

[v] Includes the vibrational contribution; see equation (32) in [57]. The electronic contribution is 9·91 au.

[w] Rizzo *et al.* give values of the molar Cotton–Mouton constant corresponding to $\Delta n_u = -1{\cdot}42 \times 10^{-13}$ at 273·15 K and $\Delta n_u = -1{\cdot}22 \times 10^{-13}$ at 293·15 K.

[x] Coupled clusters doubles.

[y] Rizzo *et al.* give a value of the molar Cotton–Mouton constant corresponding to $\Delta n_u = -3{\cdot}17 \times 10^{-13}$ at 273·15 K.

[z] Estimated.

[aa] Rizzo *et al.* give values of the molar Cotton–Mouton constant corresponding to $\Delta n_u = -2{\cdot}54 \times 10^{-13}$ at 273·15 K, $\Delta n_u = -2{\cdot}19 \times 10^{-13}$ at 293·15 K and $\Delta n_u = -2{\cdot}13 \times 10^{-13}$ at 298·15 K.

[bb] Includes the vibrational contribution; see equation (32) in [57]. The electronic contribution is 24·46 au. See also the MP3 perturbation theory (26·64 au) and the L-CCD (25·71 au) estimates of the electronic contribution in [62].

[cc] Includes the vibrational contribution; see equation (32) in [57]. The electronic contribution in 24·84 au.

[dd] Includes the vibrational contribution; see equation (32) in [57]. The electronic contribution is 25·04 au.

[ee] Includes the vibrational contribution, see equation (32) in [57]. The electronic contribution is 37·85 au. See also the MP3 perturbation theory (36·21 au) and the L-CCD (36·00 au) estimates of the electronic contribution in [62].

[ff] Includes the vibrational contribution; see equation (32) in [57]. The electronic contribution is 39.34 au.

[gg] Includes the vibrational contribution; see equation (32) in [57]. The electronic contribution is 40·14 au.

[hh] The authors give values of the molar Cotton–Mouton constant corresponding to $\Delta n_u = -2{\cdot}02 \times 10^{-13}$ at 273·15 K and $\Delta n_u = -1{\cdot}75 \times 10^{-13}$ at 293·15 K.

[ii] Estimated to within $\pm 8{\cdot}0$ au. A Cotton–Mouton constant corresponding to $\Delta n_u = +2{\cdot}44 \times 10^{-13}$ at 273·15 K is also calculated.

[jj] SCF extrapolated limit.

[kk] Obtained by using the SCF limit for the paramagnetic contribution.

6. Comparison of theory and experiment ($\Delta\eta$)

In this section we look at the $\Delta\eta$ of those species for which there are reasonably accurate calculations and, at the same time, at least some experimental, or experimentally derived, values. It is ironic that the smallest systems (fewest electrons), for which the theoretician can be most accurate, are the most challenging for the experimentalist, since for a small species the birefringence is quite tiny. This is very much the case for the rare gas helium. Accurate sum-over-states evaluations which use explicitly ECWs and include the frequency dependence or dispersion [52], give a value of $\Delta\eta = 1{\cdot}05791$ au at $\lambda = 6328$ Å (table 8). The most accurate experimental value, and there are no $\Delta\alpha$ or $\Delta\chi$ to complicate matters, is $\Delta\eta = 0{\cdot}80 \pm 0{\cdot}16$ au at 5145 Å [30]. By considering the calculated static value ($\Delta\eta = 1{\cdot}06061$ au), it is clear that the small frequency difference is not able to account for the discrepancy between theory and experiment, but the helium gas experiment is notoriously difficult. For neon (see table 8), the difference is even greater and, although the theoretical results [54, 55] are not as accurate as those for helium (they account for electron correlation through either the MP2 or the MCSCF formalism), it is unlikely that they are wrong by the factor of two, which would be necessary to bring them into line with the experimental value [29]. For argon the situation improves, most probably because the experiment is easier, and the calculated values [55, 58] at 5145 Å ($\Delta\eta = 24$–26 au) more or less fall within the experimental bounds ($\Delta\eta = 30 \pm 4{\cdot}5$ au) which are given in [18].

For molecules (table 9), there is also, generally, poor agreement between experiment and theory. However, here there is the complicating factor that $\Delta\eta$ cannot be measured directly and that the values of the polarizability and magnetizability (magnetic susceptibility) anisotropies must be used to extract $\Delta\eta$ from the experimental data on Δn. Often $\Delta\eta$ is a small contribution to Δn and may get lost in the experimental error. For H_2 and D_2 there are exceptionally accurate calculations of $\Delta\eta$, which take into account both electron correlation and vibrational effects [50]. For H_2 at $\lambda =$ 6328 Å, the experimental value [25] is 50% higher than the theoretical value but, for a different experiment [23, 24], the theoretical value lies within the experimental bounds. Theoretically, it is found that the isotopic shift, due only to vibrational effects, is small and for D_2 the $\Delta\eta$ values are only slightly smaller than those for H_2. This is corroborated by the experimental value extracted from [25], although again the value is 50% too high. It is not, however, apparent in the experiments in [23], where an enormous shift is found [24].

For N_2, CO and C_2H_2, one could say that the theoretical and experimental values of $\Delta\eta$ are in accord but, given the wide experimental error bars, this is sophistry. We can, however, on theoretical grounds, discount the experimental value given in [15] for C_2H_2 (table 9). For CH_4, the theoretical value [64], which may be improved upon, is almost in range of the experimentally determined bounds as cited in [52]. At this time it appears to us that new experimental techniques are going to be required before $\Delta\eta$ can be measured to a level which is commensurate with today's *ab initio* computations. Such techniques have been described in section 2.

7. Conclusions

The CME is an interesting and open field. The new and very sensitive apparatus designed to measure vacuum magnetic birefringence could be used effectively to perform new measurements that would allow us to solve some of the discrepancies

Table 8. Comparison of theoretical and experimental values of $\Delta\eta$ for the rare gases.

		Theory		Experiment	
Atom	Symbol	λ (Å)	$\Delta\eta$ (au)	λ (Å)	$\Delta\eta$ (au)
Helium	He	∞	1·06061[a]		
		6328	1·05791[b]	6328	1·1 ± 1·1[c]
				5145	0·80 ± 0·16[d]
Neon	Ne	6328	3·029[e]	6328	4·1 ± 3·0[c]
		5145	3·034[e]	5145	1·25 ± 0·07[f]
		5145	2·670[g]		
Argon	Ar	6328	25·68[e]	6328	26·0 ± 1·5[c]
		5145	25·70[e]	5145	30·0 ± 4·5[h]
		5145	24·14[i]		

[a] This is the static value and was obtained from a highly accurate, explicitly electron-correlated procedure [52].
[b] This is a slightly revised value of that given in [52].
[c] The value cited in [52] as a private communication from W. Hüttner.
[d] From [30].
[e] MP2 perturbation theory results from [55].
[f] From [29].
[g] MCSCF results from [54].
[h] From [18].
[i] MCSCF results from [58].

Table 9. Comparison of theoretical and experimental values of $\Delta\eta$ for some simple molecules.

		Theory		Experiment	
Molecule	Formula	λ (Å)	$\Delta\eta$ (au)	λ (Å)	$\Delta\eta$ (au)
Hydrogen	H_2	6328	10·547[a]	6328	15·7 ± 2[b]
		5145	10·386[a]	5145	9 ± 2[c]
Deuterium	D_2	6328	10·374[a]	6328	15·3 ± 3[b]
		5145	10·175[a]	5145	2 ± 3[c]
Nitrogen	N_2	6328	22·55[d]	6328	96·9 ± 75[e]
Carbon monoxide	CO	6328	37·54[d]	6328	7·5 ± 60[e]
Acetylene	C_2H_2	∞	86·85[f]	6328	20 ± 54[g]
				6328	455 ± 34[h]
Methane	CH_4	∞	40·7	6328	48·1 ± 3·0[i]

[a] Explicitly electron-correlated calculation, also all vibrational effects are included [50].
[b] From [25].
[c] Based on the experimental results in [23] as analysed by Buckingham and Williams [24].
[d] MP2 perturbation theory calculations with vibrational effects included [57].
[e] From [17].
[f] MCSCF calculation in [60].
[g] From [33].
[h] From [15].
[i] MCSCF calculation in [64].
[j] W. Hüttner, cited as a private communication in [52].

between theory and experiment for gases such as neon and helium. Computational methods are also very promising. All this should undoubtedly be a stimulus to experimentalists to push the accuracy of their results and to computational chemists to widen the range of systems that they investigate and to extend the sophistication of their techniques.

Acknowledgments

A.R. and C.R. warmly thank Michał Jaszunski, Emilio Zavattini and Erseo Polacco for long insightful discussions and a critical reading of the manuscript. A.R. also thanks Kenneth Ruud and Sonia Coriani for their invaluable help. D.M.B. acknowledges financial support from the Natural Sciences and Engineering Council of Canada.

References

[1] Cotton, A., and Mouton, H., 1905, *Ct. r. hebd. Séanc Acad. Sci., Paris*, **141**, 317, 349; 1906, *Ibid.*, **142**, 203; 1907, *Ibid.*, **145**, 229; 1907, *Ann. Chem. Phys.*, **11**, 145, 289.

[2] Kerr, J., 1901, *Br. Assoc. Rep.*, 568.

[3] Majorana, Q., 1902, *Rendic. Accad. Lincei*, **11**, 374; 1902, *Ct. r. hebd. Séanc Acad. Sci., Paris*, **135**, 159, 235.

[4] Kerr, J., 1875, *Phil. Mag.*, **50**, 337, 446.

[5] Faraday, M., 1846, *Phil. Mag.*, **28**, 294; 1846, *Phil. Trans. R. Soc.*, **1,** 136.

[6] Buckingham, A. D., Prichard, W. H., and Whiffen, D. H., 1967, *Trans. Faraday Soc.*, **63**, 1057.

[7] König, H., 1938, *Annln Phys.*, **31**, 289.

[8] Bizette, H., and Tsaï Belling, 1935, *Ct. r. hebd. Séanc Acad. Sci., Paris*, **201**, 955; 1936 *Ibid.*, **202**, 2143; 1937, *Ibid.*, **204**, 1870; 1946, *Annls Phys.*, **1**, 233.

[9] Cotton, A., and Tsaï Belling, 1934, *Ct. r. hebd. Séanc Acad. Sci., Paris*, **198**, 1889; Tsaï Belling, 1933, *Ct. r. hebd. Séanc Acad. Sci., Paris*, **195**, 1615.

[10] Buckingham, A. D., Prichard, W. H., and Whiffen, D. H., 1965, *Chem. Commun.*, **3**, 51.

[11] Corfield, M. G., 1969, PhD Thesis, University of Bristol.

[12] Bogaard, M. P., Buckingham, A. D., Corfield, M. G., Dunmur, D. A., and White, A. H., 1972, *Chem. Phys. Lett.*, **12**, 558.

[13] Geschka, H., Pferrer, S., Häussler, H., and Hüttner, W., 1982, *Ber. Bunsenges. phys. Chem.*, **86**, 790.

[14] Carusotto, S., Polacco, E., Iacopini, E., Stefanini, G., and Zavattini, E., 1982, *Optics Commun.*, **42**, 104.

[15] Kling, H., Geschka, H., and Hüttner, W., 1983, *Chem. Phys. Lett.*, **96**, 631.

[16] Kling, H., Dreier, E., and Hüttner, W., 1983, *J. chem. Phys.*, **78**, 4309.

[17] Kling, H., and Hüttner, W., 1984, *Chem. Phys.*, **90**, 207.

[18] Carusotto, S., Iacopini, E., Polacco, E., Scuri, F., Stefanini, G., and Zavattini, E., 1984, *J. opt. Soc. Am.* B, **1**, 635.

[19] Lukins, P. B., Buckingham, A. D., and Ritchie, G. L. D., 1984, *J. phys. Chem.*, **88**, 2414.

[20] Kling, H., and Hüttner, W., 1985, *Molec. Phys.*, **56**, 303.

[21] Lukins, P. B., Laver, D. R., Buckingham, A. D., and Ritchie, G. L. D., 1985, *J. phys. Chem.*, **89**, 1309.

[22] Lukins, P. B., and Ritchie, G. L. D., 1985, *J. phys. Chem.*, **89**, 1312.

[23] Scuri, F., Stefanini, G., Zavattini, E., Carusotto, S., Iacopini, E., and Polacco, E., 1986, *J. Chem. Phys.*, **85**, 1789.

[24] Buckingham, A. D., and Williams, J. H., 1987, *J. chem. Phys.*, **86**, 5883.

[25] Hüttner, W., Träuble, H., Wieland, H. U., and Müller, H., 1987, *Chem. Phys. Lett.*, **140**, 421.

[26] Lukins, P. B., and Ritchie, G. L. D., 1988, *J. phys. Chem.*, **92**, 2013.

[27] Craven, I. E., Hesling, M. R., Laver, D. R., Lukins, P. B., Ritchie, G. L. D., and Vrbancich, J., 1989, *J. phys. Chem.*, **93**, 627.

[28] Lukins, P. B., and Ritchie, G. L. D., 1991, *Chem. Phys. Lett.*, **180**, 551.

[29] Cameron, R., Cantatore, G., Melissinos, A. C., Rogers, J., Semertzidis, Y., Halama, H., Prodell, A., Nezrick, F. A., Rizzo, C., and Zavattini, E., 1991, *J. opt. Soc. Am.* B, **8**, 520.

[30] Cameron, R., Cantatore, G., Melissinos, A. C., Semertzidis, Y., Halama, H., Lazarus, D., Prodell, A., Nezrick, F., Micossi, P., Rizzo, C., Ruoso, G., and Zavattini, E., 1991, *Phys. Lett.* A, **157**, 125.

[31] Coonan, M. H., and Ritchie, G. L. D., 1991, *J. phys. Chem.*, **95**, 1220.

[32] Coonan, M. H., Craven, I. E., Hesling, M. R., Ritchie, G. L. D., and Spackman, M. A., 1992, *J. phys. Chem.*, **96**, 7301.

[33] Coonan, M. H., and Ritchie, G. L. D., 1993, *Chem. Phys. Lett.*, **202**, 237.

[34] Adler, S. L., 1971, *Ann. Phys.* (*NY*), **87**, 599.

[35] Ni, W., Tsubono, K., Mio, N., Narihara, K., Chen, S., King, S., and Pan, S., 1991, *Mod. Phys. Lett.* A, **6**, 3671.

[36] Cameron, R., Cantatore, G., Melissinos, A. C., Ruoso, G., Semertzidis, Y., Halama, H. J., Lazarus, D., Prodell, A. G., Nezrick, F., Rizzo, C., and Zavattini, E., 1993, *Phys. Rev.* D, **47**, 3707.

[37] Bakalov, D., Cantatore, G., Carugno, G., Carusotto, S., Favaron, P., Della Valle, F., Gabrielli, I., Gastaldi, U., Iacopini, E., Micossi, P., Milotti, E., Onofrio, R., Pengo, R., Perrone, F., Petrucci, G., Polacco, E., Rizzo, C., Ruoso, G., Zavattini, E., and Zavattini, G., 1994, *Nucl. Phys.* B (Proc. Suppl.), **35**, 180.

[38] Lee, S. A., Fairbank, Jr., W. M., Toki, W., Hall, J. L., Jaffery, T., Colestock, P., Cupps, V., Kautzky, H., Kuchnir, M., and Nezrick, F., 1995, Proposal submitted to Fermi National Accelerator Laboratory, Batavia, IL, USA, 28/3/1995.

[39] Langevin, P., 1910, *Radium*, *Paris*, **7**, 249.

[40] Buckingham, A. D., and Pople, J. A., 1956, *Proc. phys. Soc.* B, **69**, 1133.

[41] Kielich, S., 1962, *Acta Phys. Polonica*, **22**, 299.

[42] Atkins, P. W., and Miller, M. H., 1968, *Molec. Phys.*, **15**, 491.

[43] Chang, T. Y., 1972, *J. chem. Phys.*, **56**, 1752.

[44] Carusotto, S., Iacopini, E., Scuri, F., and Stefanini, G., 1985, *Lett. Nuovo Cim.*, **42**, 204.

[45] Buckingham, A. D., and Pople, J. A., 1957, *Proc. Camb. Phil. Soc. math. phys. Sci.*, **53**, 262.

[46] Jamieson, M. J., 1986, *Chem. Phys. Lett.*, **123**, 402.

[47] Jamieson, M. J., 1989, *Chem. Phys. Lett.*, **154**, 521.

[48] Fowler, P. W., and Buckingham, A. D., 1989, *Molec. Phys.*, **67**, 681.

[49] Jamieson, M. J., 1991, *Chem. Phys. Lett.*, **176**, 467.

[50] Bishop, D. M., Cybulski, S. M., and Pipin, J., 1991, *J. chem. Phys.*, **94**, 6686.

[51] Jamieson, M. J., 1991, *Chem. Phys. Lett.*, **183**, 9.

[52] Bishop, D. M., and Pipin, J., 1991, *Chem. Phys. Lett.*, **186**, 195; 1995, *Ibid.*, **241**, 484.

[53] Augspurger, J. D., and Dykstra, C. E., 1992, *Molec. Phys.*, **76**, 229.

[54] Jaszunski, M., Jensen, H. J. Aa., Jørgensen, P., Rizzo, A., Helgaker, T., and Ruud, K., 1992, *Chem. Phys. Lett.*, **191**, 599.

[55] Bishop, D. M., and Cybulski, S. M., 1992, *Chem. Phys. Lett.*, **200**, 153.

[56] Bishop, D. M., and Cybulski, S. M., 1993, *Chem. Phys. Lett.*, **211**, 255.

[57] Cybulski, S. M., and Bishop, D. M., 1994, *J. chem. Phys.*, **101**, 424.

[58] Jazszunski, M., Jørgensen, P., and Rizzo, A., 1995, *Theor. chim. Acta*, **90**, 291.

[59] Bishop, D. M., and Cybulski, S. M., 1994, *J. chem. Phys.*, **101**, 2180.

[60] Rizzo, A., Helgaker, T., Ruud, K., Barszczewicz, A., Jaszunski, M., and Jørgensen, P., 1995, *J. chem. Phys.*, **102**, 8953.

[61] Norman, P., Jonsson, D., Vahtras, O., and Ågren, H., 1996, *Chem. Phys.*, **203**, 23.

[62] Cybulski, S. M., and Bishop, D. M., 1996, *Chem. Phys. Lett.*, **250**, 471.

[63] Jonsson, D., Norman, P., Vahtras, O., and Ågren, H., 1996, *Theor. chim. Acta*, **93,** 235.

[64] Coriani, S., Rizzo, A., Ruud, K., and Helgaker, T., 1996, *Molec. Phys.*, **88**, 931.

[65] Coriani, S., Rizzo, A., Ruud, K., and Helgaker, T., 1996, *Chem. Phys.*, (in press).

[66] Bishop, D. M., 1994, *Adv. quant. Chem.*, **25**, 1.

[67] Böttcher, C. J. F., and Bordewijk, P., 1978, *Theory of Electric Polarization*, Vol. II, *Dielectrics in Time-Dependent Fields* (New York: Elsevier), chapter XIII.

[68] Williams, J. H., 1993, *Adv. chem. Phys.*, **85**, 361.

[69] Born, M., and Wolf, E., 1983, *Principles of Optics*, sixth edition (Oxford: Pergamon).

[70] Iacopini, E., and Zavattini, E., 1979, *Phys. Lett.* B, **85**, 151; Iacopini, E., Smith, B., Stefanini, G., and Zavattini, E., 1981, *Nuovo Cim. B*, **61**, 21.

[71] Yariv, A., 1985, *Optical Electronics*, third edition (New York: Holt, Rinehart and Winston), pp. 306 ff.

[72] Herriot, D., Kogelnik, H., and Kompfner, R., 1964, *Appl. Optics*, **3**, 523; Kogelnik,

H., and Li, T., 1966, *Proc. Inst. elect. electron. Engrs*, **54**, 1312; Herriot, D., and Schulte, H. J., 1965, *Appl. Optics*, **4**, 883.
[73] Ruoso, G., 1995, PhD Thesis, University of Padova; 1995, Istituto Nazionale di Fisica Nucleare Report No. LNL-INFN (REP) 94/95.
[74] Rempe, G., Thompson, R. J., Kimble, H. S., and Lalezari, R., 1992, *Optics. Lett.*, **17**, 363.
[75] De Riva, A. M., Zavattini, G., Marigo, S., Rizzo, C., Ruoso, G., Carugno, G., Onofrio, R., Carusotto, S., Papa, M., Perrone, F., Polacco, E., Cantatore, G., Della Valle, F., Micossi, P., Milotti, E., Pace, P., and Zavattini, E., 1996, *Rev. scient. Instrum.*, **67**, 2680.
[76] Pound, R. V., 1946, *Rev. scient. Instrum.*, **17**, 460; Drever, R. W. P., Hall, J. L., Kowalski, F. V., Hough, J., Ford, G. M., Hunley, A. J., and Word, H., 1983, *Appl. Phys. B*, **31**, 97.
[77] Kane, T. J., and Byer, R. L., 1985, *Optics Lett.*, **10**, 65.
[78] Day, T., Gustafson, E. K., and Byer, R. L., 1992, *IEEE J. quant. Electron.*, **28**, 1106.
[79] Cantatore, G., Della Valle, F., Milotti, E., Pace, P., Zavattini, E., Polacco, E., Perrone, F., Rizzo, C., Zavattini, G., and Ruoso, G., 1995, *Rev. scient. Instrum.*, **66**, 2785.
[80] Perin, R., 1988, *IEEE Trans. Magn.*, **24,** 734.
[81] Micossi, P., Della Valle, F., Milotti, E., Zavattini, E., Rizzo, C., and Ruoso, G., 1993, *Appl. Phys.* B, **57**, 95; Jacob, D., Vallet, M., Bretenaker, F., Le Floch, A., and Oger, M., 1995, *Optics. Lett.*, **20,** 671.
[82] 4 T have been reached using permanent magnets, see: Leopold, H. A., Tilak, A. S., and Potenziani, II, E., 1993, *IEEE Trans. Magn.*, **29,** 2902.
[83] Bishop, D. M., Pipin, J., and Cybulski, S. M., 1991, *Phys. Rev.* A, **43**, 4845.
[84] Bishop, D. M., and Pipin, J., 1989, *J. chem. Phys.*, **91**, 3549.
[85] Voigt, W., 1908, *Lehrbuch der Magneto- und Elektro-optik* (Leipzig: Teubner).
[86] Born, M., 1918, *Annln Phys.*, **55**, 177; 1933, *Optik* (Berlin: Springer).
[87] Volkensteyn, M. V., 1951, *Molekularnaya Optika* (Moscow: Gostekhizdat).
[88] Beams, J. W., 1932, *Rev. Mod. Phys.*, **4**, 133.
[89] Cotton, A., 1932, *Rapp. Cons. Phys. Solvay*, 418.
[90] Germann, T. E. E., and Metz, C. F., 1940, *Colorado Univ. Studies* D, **1**, 71.
[91] Partington, J. R., 1953, *An Advanced Treatise on Physical Chemistry*, Vol. IV, (London: Longmans), pp. 285 ff.
[92] Buckingham, A. D., and Pople, J. A., 1955, *Proc. phys. Soc.* A, **68**, 905.
[93] Buckingham, A. D., 1967, *Adv. chem. Phys.*, **12**, 107.
[94] Jackson, J. D., 1975, *Classical Electrodynamics*, second edition, (New York: Wiley).
[95] Bhagavantam, S., 1966, *Crystal Symmetry and Physical Properties* (New York: Academic Press).
[96] Raynes, W. T., and Ratcliffe, R., 1979, *Molec. Phys.*, **37**, 571.
[97] Buckingham, A. D., and Orr, B. J., 1968, *Proc. roy. Soc.* A, **305**, 259.
[98] Buckingham, A. D., 1955, *Proc. phys. Soc.* A, **68**, 910.
[99] Bogaard, M. P., and Orr, B. J., 1975, *International Review of Science, Physical Chemistry, Molecular Structure, and Properties*, Ser. 2, vol. 2, edited by A. D. Buckingham (London: Butterworths), p. 149.
[100] Orr, B. J., and Ward, J. F., 1971, *Molec. Phys.*, **20**, 513.
[101] McWeeny, R., 1992, *Methods of Molecular Quantum Mechanics*, second edition (London: Academic Press).
[102] Olsen, J., and Jørgensen, P., 1985, *J. chem. Phys.*, **82**, 3235.
[103] Dalgarno, A., and Kingston, A. E., 1960, *Proc. roy. Soc.* A, **259**, 424.
[104] Bishop, D. M., 1990, *Rev. mod. Phys.*, **62**, 343.
[105] Dykstra, C. E., 1985, *J. chem. Phys.*, **82**, 4120.
[106] Jameson, C. J., and Fowler, P. W., 1986, *J. chem. Phys.*, **85**, 3432.
[107] Cooley, J. W., 1963, *Math. Comput.*, **15**, 363.
[108] Cashion, J. K., 1963, *J. chem. Phys.*, **39**, 1872.
[109] Bishop, D. M., and Kirtman, B., 1991, *J. chem. Phys.*, **95**, 2646.
[110] Cybulski, S. M., and Bishop, D. M., 1994, *J. chem. Phys.*, **100**, 2019.
[111] Arrighini, G. P., Maestro, M., and Moccia, R., 1968, *J. chem. Phys.*, **49**, 882.
[112] Helgaker, T., and Jørgensen, P., 1991, *J. chem. Phys.*, **95**, 2595.

[113] London, F., 1937, *J. Phys. Radium*, **8**, 397.

[114] Hameka, H. F., 1958, *Molec. Phys.*, **1**, 203; 1959, *Z. Naturf.* a, **14**, 599; 1962, *Rev. mod. Phys.*, **34**, 87.

[115] Ditchfield, R., 1972, *J. chem. Phys.*, **56**, 5688.

[116] Lazzeretti, P., and Zanasi, R., 1996, *Molec. Phys*, **89**, 157.

[117] Mills, I., Cvitaš, T., Homann, K., Kallay, N., and Kuchitsu, K. (editors), 1993, *IUPAC, Physical Chemistry Division: Quantities, Units and Symbols in Physical Chemistry*, second edition (Oxford: Blackwell Science).

[118] Cohen, E. R., and Taylor, B. H., 1987, *Rev. mod. Phys.*, **59**, 1121.

[119] McWeeny, R., 1973, *Nature*, **243**, 196.

[120] Bishop, D. M., and Lam, B., 1988, *Phys. Rev.* A, **37**, 464.

[121] Papadopoulos, M. G., Waite, J., and Buckingham, A. D., 1995, *J. chem. Phys.*, **102**, 371.

[122] Rychlewski, J., and Raynes, W. T., 1980, *Molec. Phys.*, **41**, 843.

[123] Rychlewski, J., 1980, *Molec. Phys.*, **41**, 833.

[124] Thomas, G. F., and Meath, W. J., 1977, *Molec. Phys.*, **34**, 113.

[125] Diercksen, G. H. F., and Sadlej, A. J., 1985, *Chem. Phys. Lett.*, **114**, 187.

[126] Sekino, H., and Bartlett, R. J., 1993, *J. chem. Phys.*, **98**, 3022.

[127] Van Wüllen, C., 1992, PhD Thesis, Ruhr Universität, Bochum.

[128] Maroulis, G., 1991, *J. chem. Phys.*, **94**, 1182.

[129] Ruud, K., 1996, private communication.

[130] Maroulis, G., and Thakkar, A. J., 1990, *J. chem. Phys.*, **93**, 652.

[131] Fowler, P. W., and Diercksen, G. H. F., 1990, *Chem. Phys. Lett.*, **167**, 105.

[132] Lazzeretti, P., Malagoli, M., and Zanasi, R., 1991, *J. Molec. Struct.* (*Theochem*), **234**, 127.